Published in final edited form as:
J Med Chem. 2008 September 25; 51(18): 5506–5521. doi:10.1021/jm8002153.

Enantiomeric Propanolamines as selective *N*-Methyl-D-aspartate 2B Receptor Antagonists†

Yesim A. Tahirovic[‡], **Matthew Geballe**[‡], **Ewa Gruszecka-Kowalik**[⊥], **Scott J. Myers**[§], **Polina Lyuboslavsky**[§], **Phuong Le**[§], **Adam French**[§], **Hasan Irier**[§], **Woo-baeg Choi**[⊥], **Keith Easterling**[§], **Hongjie Yuan**[§], **Lawrence J. Wilson**[‡], **Robert Kotloski**[‖], **James O. McNamara**[‖], **Raymond Dingledine**[§], **Dennis C. Liotta**[‡], **Stephen F. Traynelis**[*,§], and **James P. Snyder**[*,‡]
Department of Chemistry, Emory University, Atlanta, Georgia, Department of Pharmacology, Emory University School of Medicine, Atlanta, Georgia, Department of Neurobiology, Duke University, Durham, North Carolina, FOB Synthesis, Inc., Emtech Bio (Emory University and Georgia Tech), Atlanta, Georgia

Abstract

Enantiomeric propanolamines have been identified as a new class of NR2B-selective NMDA receptor antagonists. The most effective agents are biaryl structures, synthesized in six steps with overall yields ranging from 11–64%. The compounds are potent and selective inhibitors of NR2B-containing recombinant NMDA receptors with IC_{50} values between 30–100 nM. Potency is strongly controlled by substitution on both rings and the centrally located amine nitrogen. SAR analysis suggests that well-balanced polarity and chain-length factors provide the greatest inhibitory potency. Structural comparisons based on 3D shape analysis and electrostatic complementarity support this conclusion. The antagonists are neuroprotective in both in vitro and in vivo models of ischemic cell death. In addition, some compounds exhibit anticonvulsant properties. Unlike earlier generation NMDA receptor antagonists and some NR2B-selective antagonists, the present series of propanolamines does not cause increased locomotion in rodents. Thus, the NR2B-selective antagonists exhibit a range of therapeutically interesting properties.

Introduction

Glutamate, the principal excitatory neurotransmitter in the central nervous system (CNS), activates at least three subtypes of ionotropic receptors classified by agonist pharmacology as follows: *N*-methyl-D-aspartate (NMDA[a]), α-amino-3-hydroxy-5-methyl-4-isoxazole propionic acid (AMPA), and kainate receptors. [1–3] NMDA receptors are Ca^{2+} permeable ligand-gated ion channels that are activated after binding of the coagonists glutamate and

†Several of the authors (Y.A.T., J.P.S., D.L., R.D., S.F.T., J.O.M.) are inventors of Emory University owned patent-pending technology associated with these compounds, or have an equity position in companies actively seeking to license these compounds (JPS, DL, RD, SFT)

* To whom correspondence should be addressed. For S.F.T.: Phone, +1-404-727-0357; Fax, +1-404-727-0365; strayne@emory.edu. For J.P.S.: Phone, 404-727-2415; Fax, +1-404-727-6586; jsnyder@emory.edu.
‡Department of Chemistry, Emory University.
§Department of Pharmacology, Emory University School of Medicine.
‖Department of Neurobiology, Duke University.
⊥FOB Synthesis, Inc., Emtech Bio (Emory University and Georgia Tech).

Note Added after ASAP Publication. This manuscript was released on August 23, 2008 with an error in Figure 1. The correct version was posted on September 18, 2008.

Supporting Information **Available:** Spectral information and elemental analysis for compounds. This material is available free of charge via the Internet at http://pubs.acs.org.

glycine. These ion channels mediate excitatory transmission in the CNS and also play an important role in synaptic plasticity. Under pathological conditions, overactivation of NMDA receptors has been hypothesized to contribute to neuronal death, in part by elevating intracellular divalent ions such as Ca^{2+} and Zn^{2+} to cytotoxic levels. Given these important roles for this receptor, there has been a great deal of interest in developing pharmacologic regulators of this receptor class. [4–7]

NMDA receptors are heterooligomeric assemblies of NR1 subunits plus one or more NR2A, NR2B, NR2C, and NR2D subunits.[1,2,8–10] Subunit composition and distribution of native receptors in adult mammalian brain differs significantly from region to region.[11] In addition, each subunit contributes uniquely to gating, and binds different agonists and allosteric regulators.[2] The NR1 subunit contains the glycine binding site, whereas the NR2 subunit contains the glutamate binding site.[2] In addition, NR2 subunits possess binding sites for allosteric regulators and noncompetitive antagonists such as extracellular Zn^{2+} and phenylethanolamines such as ifenprodil.[12–15] This varied NMDA receptor pharmacology provides an opportunity to develop subtype-selective therapeutic drugs.[8–11]

One of the first subtype-selective NMDA receptor antagonists was ifenprodil, which selectively inhibits NR2B-containing NMDA receptors.[16] A wide range of ifenprodil analogues have been synthesized, including eliprodil[17] and other benzylpiperidines (**111**[20] and **112**,[18,19] Figure 1). Several additional classes of NR2B-selective NMDA receptor antagonists also have been described including oxamides,[21] 5-substituted benzimidazoles,[22] indole-2-carboxamides,[23] benzyl cinnamamidines,[24] and other biaryl analogues[25,26] (see Figure 1).

We describe here a structurally distinct class of enantiomeric propanolamines that are potent antagonists of NR2B-containing NMDA receptors. The compounds are both neuroprotective and anticonvulsant when tested in vivo.

Synthesis

As shown in Schemes 1 and 2, syntheses of compounds **29–43** (Table 1) were initiated by combining substituted nitrophenols with (*S*)-(+)-glycidyl nosylate under basic conditions using the procedure described by Kitaori et al.[27] to give **2–8** in excellent yields (80–93%). The latter were hydrogenated with poisoned Pd/C[28] using a previously published procedure[29] to obtain crude mixtures resulting from nitro group reduction and 5–20% ring opening. As a result of instability on silica gel, the reduced product mixtures were used directly without purification. Thus, **9–14** were treated with *N*,*N*-diisopropyl-*N*-ethyl amine and the corresponding acid chloride (iii or iv in Scheme 1) to produce compounds **15–27** in moderate yields. Methyl iodide and potassium carbonate in acetone were subsequently used to methylate the sulfonylamide nitrogen to give **28**. Finally, the side chain was elaborated by opening the epoxide ring with 3,4-dichlorophenylethylamine to furnish **29–42** (i.e., via v in Scheme 1).

[a]Abbreviations: nM, nanomolar; μM, micro molar; mM, millimolar; hERG, human ether-a-go-go; MCAO, middle cerebral artery occlusion; NMDA, *N*-methyl D-aspartate; AMPA, α-amino-3-hydroxy-5-methyl-4-isoxazole propionic acid; ROCS, rapid overlay of chemical structures; EON, electrostatic potential maps; NR2B, *N*-methyl D-aspartate receptor 2B subunit; ATD, amino terminal domain; ANOVA, analysis of variance; mg, milligram; kg, kilogram; min, minute; ip, intraperitoneal; LC, liquid chromatography; MS, mass spectroscopy; TLC, thin layer chromatography; NMR, nuclear magnetic resonance; DMSO, dimethylsulfoxide; Hz, hertz; mmol, millimole; DMF, dimethylformamide; mL, milliliter; HPLC, high pressure liquid chromatography; MHz, megahertz; THF, tetrahyrofurane; μm, micrometer; DCM, dichloromethane; MeOH, methanol; MMFF, Merck molecular force field; cRNA, complementary RNA; cDNA, complementary DNA; HEPES, 4-(2-hydroxyethyl)piperazine-1-ethanesulfonic acid; NR1, *N*-methyl D-aspartate receptor 1; NR2, *N*-methyl D-aspartate receptor 2; M, molar; EDTA, ethylenediaminetetraacetic acid; D-APV, D-(–)-2-amino-5-phosphonopentanoic acid; CNQX, 6-cyano-7-nitroquinoxaline-2,3-dione; LDH, lactate dehydrogenase; ACSF, artificial cerebrospinal fluid; TTC, 2,3,5-triphenyltetrazolium chloride; PBS, phosphate buffered saline; cm, centimeter; PEG, polyethylene glycol; nA, nanoamps; MRM, multiple reaction monitoring mode.

The synthesis of **43** is shown in Scheme 2. Compound **44** was prepared by the method employed for compound **42** but starting with 2-nitrophenol. To protect both the free amine and the alcohol groups, **44** was treated with benzaldehyde in toluene followed by hydrogenation of the nitro moiety to the corresponding amine (**46**) with Pd/C (10%). Without purification, the resulting aniline was combined with methanesulfonyl chloride under basic conditions at 0 °C and subsequently treated with HCl to give compound **43** in 43% yield.

The reaction of compound **15** and the appropriate primary or secondary amine in ethanol gave compounds **47–65** (Table 2) as shown in Scheme 3. Compounds **67–102** (Tables 3 and 4) were synthesized by reductive amination from **29** under mild conditions as shown in Scheme 4. For example, **37** was prepared in two steps. In the first step, **29** was combined with the *O*-butyryl glycoaldehyde[30] and reduced to the corresponding amine with sodium triacetoxyborohydride (**68a**), while in the second step, it was hydrolyzed with sodium methoxide to deliver **68** (75% yield). Generally, reductive amination with alkyl aldehydes gave higher yields than the aromatic aldehydes. Compounds **103–108** are the (*R*) mirror-image isomers of **29**, **66**, **68**, **70**, **76**, and **77**. They were prepared similar to the latter compounds starting with the (*R*)-glycidyl nosylate. To illustrate the enantiomeric purity of the compounds, we selected enantiomers **70** and **106** and prepared the corresponding Mosher esters. The clean singlet peak for the methoxy group in each case indicates that the compounds are enantiomerically pure. The corresponding optical rotations ($[\alpha]_D^{20}$) are −12.6° and + 12.7°, respectively. Experimental details and the NMR spectra of the Mosher esters are provided in the Supporting Information.

In Vitro Analysis of NMDA Receptor Antagonism

Two electrode voltage clamp recordings from *Xenopus* oocytes expressing recombinant rat NMDA receptors were used to test for subunit selective inhibition by all experimental compounds (Tables 1–6). From these experiments, we determined that **29** is a novel, potent, and selective antagonist at recombinant rat NR1/NR2B receptors (Figure 2A,B). Two additional closely related compounds (racemic **66**/**104**) were similarly potent and differed from **29** only by addition of a methyl group. Racemic **66/104** (AM-92016) is a potassium channel blocker.[31] All three compounds (**29**, **66**, **104**) were used interchangeably to evaluate the mechanism by which propanolamines inhibit NR2B-containing recombinant NMDA receptors. In addition, these three compounds were tested in a number of in vitro and in vivo models of ischemia, epilepsy, and locomotor activity.

Compound **29** inhibits rat NR1/NR2B current responses with a half-maximally effective concentration of 50 nM (Hill slope 0.7); **29** showed a similar potency for inhibiting human NR1/NR2B receptors (53 nM). Furthermore, the amino acid identity between rodent and human receptors is 98% or better with most changes occurring in a region of the receptor not expected to be part of the binding pocket for NR2B-selective inhibitors. All subsequent experiments reported were performed on rat NMDA receptors. Interestingly, **29** did not inhibit receptor function fully but rather showed a maximal inhibition of only 83%. The latter is consistent with that of other NR2B-selective antagonists, which act by a noncompetitive mechanism to bring about incomplete inhibition.[16,19,20,32–34] Compound **29** has no effect on recombinant heterodimeric NMDA receptors that contain other NR2 subunits and no detectable effects on recombinant kainate or AMPA receptors (Figure 2A). Furthermore, consistent with other NR2B-selective ligands, inhibition of NR1/NR2B receptor responses by **29** was not surmountable by increased concentrations of glycine or glutamate (Figure 2C). Inhibition with a similarly potent analogue (racemic mixture of **66**/**104**) was voltage-independent (Figure 2D). Two mutations that have been shown to reduce ifenprodil inhibition in NR1/NR2B receptors[35,36] also blocked the inhibitory effects of **66/104**. We found that inhibition produced by a single concentration of **66/104** (100 nM)

was reduced from 67.1 ±1.1% in wild type NR1/NR2B receptor to 8.9 ± 5.6% in NR1(H134A)/NR2B ($n = 5$; $p < 0.05$; unpaired t test) and 4.2 ± 6.3% in NR1/NR2B(E201R) ($n = 7$; $p < 0.05$; unpaired t test).

These data are all consistent with propanolamine **29** and its analogues exerting a negative allosteric effect on NR2B receptor function through direct interaction with at least a portion of the ifenprodil binding site, which has been proposed to be fully contained in the amino terminal domain.[15,36,37] To directly test whether **29** and its analogues bind to the amino terminal domain, we evaluated a mouse NR2B subunit in which residues of the amino terminal domain up to Met394 were replaced by a signal sequence of influenza hemaglutinin followed by an eight residue FLAG epitope followed by the sequence TRYMRHAVWPR.[38] We hypothesized that deletion of the amino terminal domain from this NR2B subunit, NR2B (ΔATD), would render the receptors insensitive to inhibition by **29** and its analogues. Functional properties of this deletion construct are similar to that of wild-type receptors, suggesting that receptor function and structure remain largely intact (data not shown). As expected, **29** (0.3–3 mM) had no significant effect on the current response of NR1/NR2B(ΔATD) when activated by maximal concentrations of glutamate and glycine (102.5 ± 4.5% of control in 3 μM **29**; $n = 7$).

Structure–Function Relationships

An SAR for the propanolamines has been constructed by modifying substituents of the two terminal phenyl rings and the central nitrogen as shown in **109**.

The IC_{50} values for compounds with varying substitutions on the phenoxy ring (**109**, R_1 and R_2) illustrate a remarkably strong preference for a *para*-methylsulfonamide (Table 1). Movement of the latter to the *meta* position reduces the potency assessed in the oocyte assay by 10-fold, while *ortho* placement depletes activity altogether. Similarly, hydrophobic sulfonamide substituents larger than methyl decrease potency by >10-fold, the larger groups causing the greater loss. Replacement of the sulfonamide with *N*-acetyl analogues or a nitro group reduces the IC_{50} >100-fold, as does *N*-methylation. Once the *p*-$NHSO_2Me$ is installed, an *ortho*-F is well tolerated, but *meta* substitution reduces potency by 10-fold. At the other end of the molecule, 3,4-substitution of the phenethyl moiety by combinations of fluorine and chlorine **(109,** X_1 and X_2) furnish the lowest IC_{50} values (i.e., highest potency Table 2). However, a 5–15 fold drop in potency is produced by either the difluoro or dimethyl variations, removal of one of the halogens or F or C at C-2. A variety of other substituents, most notably OH and NO_2, lead to greater than 100-fold decrease in potency (i.e., increase in IC_{50}). Although the terminal groups have been limited to phenyl rings, within this context the range of acceptable changes is limited to a rather tight pattern: 4-methyl-sulfonamide on the right and 3,4-dichloro on the left. Compound **29** with an IC_{50} of 50 nM corresponds to the lead structure.

Further modifications have focused on the amine nitrogen located unsymmetrically between the aromatic termini (**109**, R_3). Within a series of alkyl derivatives there is a clear size preference. The ethyl group and the corresponding alcohol are optimal with only 2–3 fold less activity than **29**. However, both the small methyl group and substituents with 3–6 carbons exhibit 3–13 fold lower activity (Table 3). The even bulkier isobutyl and cyclohexylmethyl groups drop the potency further relative to the *N*-ethyl analogue, namely 13–100 fold. Analysis of the seven *N*-substituted propanolamines (**29**, **66**, **67**, **69–72**) shows a correlation between spacefill volume of the side chain and potency ($R = 0.92$, $p < 0.004$), with more sharply decreasing potency beyond *n*-propyl. The existence of a pocket with limited size that can accommodate these aliphatic substituents is suggested. A series of *N*-benzyl derivatives was likewise prepared, many of which retain potencies in the 200–500 nM range (Table 4). Small substituents such as F, OH at all positions are tolerated (IC_{50}

values 200–500 nM), including 2,3,4-triflluoro, which has similar potency to **29** (51 nM). Larger moieties on the ring (CH_3, CF_3 and C-2 OMe) dampen the activity, as do phenethyl analogues. A limited treatment of heterocyclic derivatives ($HetCH_2$) indicates a sampling of IC_{50} values in the 200 nM to 4 μM range.

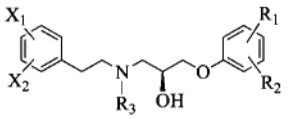

109

Lastly, the alcohol group located in the propanolamine fragment creates a stereogenic center. The enantioselectivity for several representative class members is shown in Table 5. The striking outcome is that for five pairs of enantiomers, the IC_{50} *R/S* ratios vary from 1–3. That is, alcohol configuration is not an important determinant of potency. The single possible exception corresponds to the enantiomers of **29**, the most active series member with an enantiomeric ratio of 3.8. Given the narrow window of differences, these observations would seem to be one of the many exceptions to Pfeiffer's rule, which states that the higher the activity of a eutomer, the higher the separation in activities between eutomer and distomer.[39] The receptor pocket that houses this class of molecules is most likely endowed with a geometry that accommodates the alcohol stereogenicity while binding the remaining sectors of the antagonists in a common fashion.[40,41]

Shape Comparisons with Ifenprodil

Six members of the propanolamine series and ifenprodil were examined computationally for their similarity in molecular shape and electrostatic potential. Each of the structures listed in Table 6 was subjected to a conformational search using the OMEGA conformation generator.[42] These conformer pools were then analyzed with the programs ROCS and EON.[43,44] ROCS (Rapid Overlay of Chemical Structures) provides a measure of molecular shape complementarity through maximization of shape overlap between two structures. Shape complementarity is calculated by means of a simple Tanimoto comparison (T_s) resulting in a score between 0 (no overlap) and 1.0 (identical shape). A score of $T_s > 0.7$ signifies significant shape complementarity.[45,46] EON provides a similar comparison in terms of the electrostatic potential distribution overlap between two structures. However, because the procedure does not presently allow optimization of the overlap, EON was applied directly to a set of ROCS-aligned structures. EON Tanimoto scores range from – ⅓ to 1. A similarity score of $T_e > 0.2$ is considered a significant electrostatic match.[45,46] Table 6 lists the highest scoring conformation derived from each of the propanolamines and ifenprodil after ROCS and EON comparison of OMEGA-generated conformer pools with a template conformation of **67**. The latter was selected as the template structure following a docking study of **67** to identify a proposed ligand–protein binding complex on a homology model of the NR2B ATD subunit. This work will be reported in due course.[47] The combined shape and electrostatic similarity between template and each of the query compounds is depicted by a structural overlay in Figure 3, while the electrostatic potential maps of the corresponding conformations are represented in Figure 4. This analysis identified at least one conformation for each of the query compounds that provides a significant match ($T_e >$ 0.2) to the electrostatic properties of the query conformation of **67** (Table 6). The only exception to a significant shape score within the propanolamine series is **91**, the low score ($T_s = 0.54$) a result of an extra phenyl group by comparison with other members in the set. Nonetheless, the corresponding conformation is still capable of an excellent match on the basis of electrostatic characteristics ($T_e = 0.41$). Even with inversion of the hydroxyl stereocenter (compound **103**), a significant correlation of both shape and electrostatic signatures ($T_s = 0.72$, $T_e = 0.36$) is achieved, perhaps explaining the surprising lack of

sensitivity to inversion at this location. The shape comparison for ifenprodil (T_s = 0.68) puts it below (but close to) the threshold for a significant shape similarity. Nonetheless, the substantial electrostatic similarity (T_e = 0.20) denotes a degree of similarity between these two scaffolds despite their atomic differences.

The propanolamine similarity comparisons imply that although changes can be made to multiple regions of the molecular scaffold, by and large the structures retain the ability to access similar conformations and present comparable electrostatic signatures to their surroundings. A degree of complementarity with ifenprodil supports the notion that the propanolamines and ifenprodil may access a common binding site.

Off-Target effects of 29

Compound **29** had no significant effect on neuronal voltage-activated currents. Tetrodotoxin-sensitive neuronal Na^+ currents recorded at −10 mV were 1.31 ± 0.20 nA in control and 1.27 ± 0.18 nA in 3 μM **29** (n = 5; p = 0.23; paired t test). Voltage-gated K^+ currents were 0.72 ± 0.13 nA in control and 0.72 ± 0.13 nA in 3 μM **29** (n = 6; p = 0.66; paired t test). The current–voltage relationships for Na^+ and K^+ currents were superimposable at all potentials (data not shown). Additional studies show that **29** does not bind to L-type or N-type calcium channels or to sodium channels (IC_{50} values > 5–10 μM; data not shown). As with other classes of NR2B-selective antagonists,[3,48] **29** binds hERG channels with an IC_{50} of 0.73 μM, which is ~15-fold higher the than IC_{50} for inhibition of NR1/NR2B receptors (0.050 μM, n = 53). The hERG IC_{20} for **29** is 174 nM. Compound **29** also shows limited binding to α-1 and α-2 adrenergic receptors with IC_{50} values of 2.4 μM and >3 μM, respectively, as well as the serotonin transporter (>3 μM). However, binding to dopamine and norepinephrine transporters was more potent, with estimated IC_{50} values around 0.5 μM. Binding to both hERG and α-1 adrenergic receptors can be modulated by changing the R_1 substitution of the phenyl ring in the 3 and/or 4 position (Table 7). A substituted benzyl group at the R_2 position reduces both hERG and α-1 adrenergic binding. In addition, α-1 adrenergic binding is systematically reduced by the R_2 group when substitution is alkyl (Table 7), whereas these same substitutions have varying effects on hERG binding. The latter suggests that the size of the amine aliphatic substitution can influence hERG binding.

In Vitro and in Vivo Analysis of Neuroprotection

NMDA receptor overactivation during neuropathological insult has long been considered an important contributor to the sequence of events that leads to cell death.[49–51] For this reason, there has been interest in utilizing NMDA receptor antagonists as potential neuroprotectants for conditions such as ischemic stroke. Initial clinical trials of competitive NMDA receptor blockers as well as channel blockers failed for a number of reasons, including unfavorable side effect profile, dose lowering in an effort to avoid negative side effects, and the inability to administer the compounds early enough after the ischemic event to prevent NMDA receptor-mediated cell death. The latter is thought to occur in the initial hours post ischemia. To avoid some of these problems, subunit selective antagonists have been developed and pursued in both in vitro and in vivo models of neuronal injury. We therefore tested propanolamine **29** as a representative of this class for neuroprotective actions in two of the most common models of NMDA receptor mediated excitotoxicity: NMDA-mediated neurotoxicity of cultured rat cortical neurons[52,53] and the transient focal ischemia produced by occlusion of the middle cerebral artery (MCAO) model[54,55] in mice.

Figure 5A summarizes data showing that propanolamine **29** is neuroprotective against NMDA receptor mediated cell death in vitro. Cortical neuronal cultures were exposed for 10 min to 100 μM NMDA and 10 μM glycine to activate NMDA (but not kainate or AMPA)

receptors selectively. For each experiment, a subset of cultures were treated with NMDA/glycine plus varying concentrations of propanolamine **29**. Cultures were subsequently washed with saturating concentrations of a non-selective antagonist cocktail that can block all glutamate receptors (APV, CNQX, see Methods). The culture media was replaced and returned to the incubator for 24 h. After this time, a spectrophotometric assay was performed to measure release of the stable intracellular enzyme lactate dehydrogenase. This approach is a widely used, reliable measure of cell injury because a robust correlation exists between cell death and LDH release. Figure 5A shows the extent of neuronal death induced by NMDA treatment as well as the concentration-dependent ability of **29** to reduce cell death, assessed through release of LDH. Our interpretation of these data is that propanolamines prevent cell death in cultured neurons caused by overactivation of NR2B subunit-containing native NMDA receptors.

We subsequently tested the effects of **29** on ischemia-induced neuronal death in vivo using the MCAO model of transient focal ischemia. Occlusion of the middle cerebral artery was performed in C57Bl/6 mice for 30 min, followed by survival for 24 h. At this time, animals were sacrificed, and the brain cut into 2 mm sections and stained for viable cells using 2,3,5-triphenyltetra-zolium chloride (TTC). Figure 5B shows two sections from mice pretreated with either 30 mg/kg of propanolamine **29** ip or vehicle. The infarct volume, which is shown in red, is outlined by a thresholded digital measurement of >30% reduction in staining intensity. It is clear from these data that **29** is neuroprotective. The right panel summarizes measurements from a large number of animals and shows a significant reduction in infarct volume that is caused by preinjection of **29** at 30 mg/kg ($p < 0.05$, Mann–Whitney). These data are consistent with results showing other NR2B-selective antagonists are neuroprotective.[6,55,56] In addition, it seems unlikely that potential potassium channel blockade by **29** would be neuroprotective because this should lead to further depolarization of neurons, spike firing, and additional glutamate release. Peak brain concentration of **29** (0.17 μM, see below) is 3 times the IC_{50} for block of NMDAR but insufficient to fully block mouse hERG channels.

In Vivo Analysis of Anticonvulsant Activity

It has long been known that NMDA receptor activators induce seizures and that NMDA receptor antagonists can be anticonvulsant.[57,58] Moreover, NR2B-selective NMDA receptor antagonists have shown some anticonvulsant activity in animal models of epilepsy.[59,60] We therefore sought to test whether the novel compounds described here are anticonvulsant in an in vivo model of electrographic seizures. Figure 5C summarizes data showing the effects of **29** and **68** or a racemic mixture of compounds **66/104** administered ip at 30 mg/kg on the duration of tonic hind limb extension during electroshock induced seizures in rats. Both **68** and racemic **66/104** (30 mg/kg) significantly reduced tonic hind limb extension (Figure 5C). Although 30 mg/kg of the prototypical **29** did not significantly reduce tonic hind limb extension (Figure 5C), a higher dose of **29** (100 mg/kg) significantly reduced tonic hind limb extension duration (68 ± 6.1% of control; $p < 0.001$; $n = 10$). A reduction in tonic hind limb extension in the electroshock model is a predictor of clinical effectiveness for drugs of diverse structure.[61]

In Vivo Analysis of Locomotor Activity and Rotorod Performance

Although NMDA receptor antagonists are neuroprotective and anticonvulsant, one persistent complication that has impeded clinical development has been a number of serious side effects associated with blockade of NMDA receptors, which include psychosis and ataxia.[62–64] One reliable in vivo test of side effects is the ability of NMDA receptor antagonists to influence locomotor activity, with low doses increasing locomotor activity and the highest doses producing complete ataxia.[65,66] Figure 6A shows the locomotor-

stimulating activity of nonselective NMDA receptor channel blockers like aptiganel and competitive antagonists such as selfotel (* $p < 0.05$, ANOVA, posthoc Dunnett's). Some NR2-selective antagonists (e.g., **111**, Figure 1) increase locomotion,[67,68] although propanolamines in the series developed here, as characterized by **29**, show virtually no effect on locomotor activity at doses (300 mg/kg) that are at least ten times greater than an effective neuroprotective dose (30 mg/kg). Ifenprodil impaired locomotor activity at high doses. Three of the four animals in our study died at 300 mg/kg dosages of ifenprodil. These data show that propanolamines induce less locomotor activity changes than other well-studied NR2B-selective antagonists as well as nonselective NMDA receptor antagonists. The lack of locomotor activity of propanolamines compared to the Ro compound (Figure 1) could be due to either unique pharmacokinetic properties, unknown interactions with nonglutamate receptor targets in brain, differences in the magnitude of percent maximal block of NR2B receptors, or differences of other features of the effects of **111** (Figure 1) on NR1/NR2B receptor function.

In addition, mice were tested for motor coordination in a rotorod assay in Figure 6B. Mice were placed on a rotating spindle that was accelerated from 3 to 35 rpm over 5 min and the latency to fall was recorded. Mice were tested four times each day for five days (within day intertrial intervals were 25 min). On day five mice were injected ip with 30 mg/kg **29** 20 min prior to the first trial. Like vehicle, **29** does not impair performance on the rotorod. Injection of the potent, nonselective NMDA antagonist **110** ((+)MK-801)[64–66] at 0.3 mg/kg, however, results in a significant impairment in performance that reverses over time, most likely due to clearance of drug from the animals. A higher dose of **110** (0.6 mg/kg) results in complete ataxia, and animals are unable to perform the rotorod test on day 5 (not shown).

Plasma and Brain Levels of Propanolamines

In vivo efficacy for **29**, **66**, and **104** already suggests that these compounds cross the blood–brain barrier and persist at significant levels for at least 30 min. To verify that other members of this class of NR2B-selective antagonist are bioavailable, we evaluated plasma half-life and brain/plasma ratio for a range of structurally similar compounds with varied substitution on the chain nitrogen. Compounds **67**, **68**, **70**, **77**, and **98** were administered to rats intravenously (4 mg/kg; $n = 3$) and **29** administered at 30 mg/kg ip, and the plasma levels of compounds measured by LC-MS/MS at multiple time points (5, 30, 60, 120, and 240 min) following administration (see Methods). The $t_{1/2}$ (plasma half-life) for these compounds ranges from 0.6 to 1.2 h (**29** = 1.1 h). There is no apparent correlation of the terminal half-life with the size of the amino alkyl substitution. Compound **70** penetrates brain well with brain to plasma ratios of 1.1, whereas **29** has a lower brain to plasma ratio (<0.05). Both brain/plasma ratios were relatively constant over time. Because **29** and **70** have similar overall structural features, such as the dichlorophenethyl propanolamine and methane sulfonamide, the reasons for the differences in brain penetration are not obvious. However, the combination of lower total polar surface area (78 versus 87) and higher ClogP (5.3 versus 3.1) for **70** versus **29** may play a role. Following a 30 mg/kg ip dose of **29**, brain levels peaked at 0.17 μM or three times the IC_{50} for block of NMDAR as measured in the oocyte assay. Interestingly, brain concentrations are sustained even as plasma levels fall by over 4-fold. Thus, at doses of **29** administered for transient ischemia, occupancy of NR2B receptors by **29** may exceed 60% for 2 h post surgery. Accounting for mouse plasma binding of 88% (98% in human plasma), the free concentration of **29** in plasma during the ischemic episode ranged from 1 to 3 μM, and thus plasma levels are 2–3 fold above the IC_{50} for hERG binding. Although free concentrations of drug in humans could be lower, **29** exhibits a projected cardiovascular safety margin that is unsuitable as a neuroprotectant in man. Compound **29**, however, remains a valuable pharmacological tool for investigating the role of NR2B receptors in vitro and in preclinical animal studies. Oral bioavailability was not

directly measured, but computational methods (QikProp)[77] applied to compounds across the series predict **29** and racemic **66**/**104** to have moderate oral absorption potential (>30%) across the GI/blood barrier. This prediction fits with the observed pK_a values for **29**. The pK_a for the amino and sulfonamide groups was determined to be 9 and 8, respectively. On the basis of these numbers, the salt form of this compound should be dominant at low pH values, but in equilibrium with the free base at higher pH ranges (6–8).

Summary and Conclusions

In this study, we describe a series of NR2B selective NMDA receptor antagonists with a number of unique features. A diverse range of propanolamine derivatives can be prepared as pure enantiomers by straightforward procedures with 11–64% yields in six steps. The compounds are similar to the previously described prototypical class of phenylethanolamines in that they are biaryl structures with a nitrogen-containing chain. However, a significant departure from the structure–activity relationship for ifenprodil and its analogues is observed. There is a very strict requirement for substituents on the terminal aryl rings. For example, only minor variations of the 3,4-dichloro moiety on the phenylethyl ring and the 4-methylsulfonylamide moiety at the distal phenyl ring are tolerated. Various alkyl and benzyl nitrogen substituents reduce activity only slightly relative to parent **29**, but sufficiently bulky groups reduce potency drastically. Remarkably, the active enantiomers of **109** differ in their in vitro potencies with low eutomer/distomer ratios of 0.7–3.8. This observation implies a forgiving binding pocket. Molecular templating of a selection of the most active analogues confirms that the series can adopt a common 3-D shape and hydrophobic–hydrophilic profile. It also provides insight into the diminished *R/S* ratios by suggesting that molecular profile is altered very little by inversion at the C-OH stereogenic center.

These potent subunit-selective antagonists display a number of intriguing activities in vivo. For example, they are neuroprotective in a mouse model of transient focal ischemia. Compound **29** decreased infarct volume when administered before an ischemic episode. Moreover, some of the compounds were shown to be anticonvulsant in the electroshock model of tonic clonic seizures. These two properties are consistent with results from other NR2B-selective antagonists, raising interest in therapeutic exploitation of this class of compound. Propanolamines in this structural series that were tested appear to show little propensity to stimulate locomotor activity, suggesting they may exhibit a reduced side effect profile. If NR2B-selective receptors can be found that are well tolerated, they should prove to be effective therapeutics for a wide range of ischemic insults. NR2B receptor antagonists have not been studied exhaustively in models of epilepsy, however, they are effective at reducing seizures in a subset of animal models of epilepsy, suggesting that these compounds may be effective anticonvulsants in some types of human epilepsy.

Experimental Section

Chemistry. General Procedures

All reagents were obtained from commercial suppliers and used without further purification. Reaction progress was monitored by thin layer chromatography (TLC) on precoated glass plates (silica gel 60 F254, 0.25 mm thickness) purchased from EM Science. Flash chromatography was carried out with silica gel 60 (230–400 mesh ASTM) from EM Science. ^{1}H NMR and ^{13}C NMR spectra were recorded on a Varian 400 spectrometer. Unless otherwise specified, all NMR spectra were obtained in deuterated chloroform ($CDCl_3$) or deuterated dimethylsulfoxide (DMSO-d_6) and referenced to the residual solvent peak; chemical shifts are reported in parts per million and coupling constants in hertz (Hz). Mass spectra were obtained on either a VG 70-S Nier Johnson or JEOL mass spectrometer.

Elemental analyses were performed by Atlantic Microlab (Norcross, GA) for C, H, and N and agreed with the proposed structures within ± 0.4% of the theoretical values.

General Method For Preparation of (*S*)-Glycidyl Substituted Nitrophenyl Ether

Substituted nitrophenol (6.6 mmol) was dissolved in 5 mL anhydrous DMF. Cesium fluoride (19.9 mmol) was added to the reaction. The reaction mixture was stirred for 1 h at room temperature, and (*S*)-glycidyl nosylate (6.6 mmol) was added to the reaction mixture. The reaction stirred for 24 h at room temperature. Water (150 mL) was added; the solution was extracted with ethyl acetate. The organic phase was dried over $MgSO_4$ and evaporated. The residue was purified with column chromatograph using ethylacetate: hexane (50:50) solvent system to give the desired product.

(*S*)-Glycidyl 4-Nitrophenyl ether (2)

(93% yield, 99.6% ee, based on chiral HPLC with Chiralcel OD, mp 78–9 °C) as a yellowish solid. The NMR values are the same as those previously reported.[27] ^{1}H NMR (400 MHz, $CDCl_3$) δ2.78 (1H, dd, J = 2.6, 4.9 Hz), 2.95 (1H, t, J = 4.2 Hz), 3.39 (1H, m), 4.0 (1H, dd, J = 5.9, 11.2 Hz), 4.38 (1H, dd, J = 2.6, 11.1 Hz), 6.99 (2H, dd, J = 2.4, 6.8 Hz), 8.2 (2H, dd, J = 2.4, 6.8 Hz).

General Method For Preparation of (*S*)-Glycidyl Amino Substituted Phenyl Ether

(*S*)-Glycidyl substituted nitrophenyl ether (2.6 mmol) and 5% Pd/C(en) (10% of the weight of starting material) in 5 mL anhydrous THF was hydrogenated at ambient pressure and temperature for 3–5 h. The reaction mixture was filtered by using membrane filter (13, 0.22 μm) and the filtrate was concentrated in vacuum. The compound was afforded as a crude mixture of amino reduction and ring opening. The isolation of the compound was difficult because of the liability of the components of the mixture on silica gel. The product ratio of the amino reduction, and ring opening was determined on the basis of the integration ratio of the epoxidering protons of amino reduction compound and the methyl proton (δ = 1.25, d, J = 6.4 Hz) of ring opening compound.

(*S*)-Glycidyl 4-Aminophenyl Ether (9)

The product ratio of the amino reduction and ring opening was 94:6 (98% yield). The NMR values are the same as those previously reported.[29] ^{1}H NMR (400 MHz, $CDCl_3$) δ 2.69 (1H, dd, J = 2.4, 4.5 Hz), 2.83 (1H, t, J = 4.5 Hz), 3.26–3.30 (1H, m), 3.43 (2H, brs), 3.83 (1H, dd, J = 5.9, 11.1 Hz), 4.1 (1H, dd, J = 3.1, 11.1 Hz), 6.59 (2H, dd, J = 2.4, 6.8 Hz), 6.72 (2H, dd, J = 2.4, 6.8 Hz).

General Method For Preparation of (*S*)-Glycidyl *N*-Alkyl/arylsulfonyl-amino-Substituted Phenyl Ether

(*S*)-Glycidyl amino substituted phenyl ether (2.4 mmol) dissolved in 20 mL anhydrous DCM and *N*,*N*-diisopropyl-*N*-ethylamine (2.6 mmol) was added at 0 °C. After stirring 15 min, alkyl/arylsulfonyl chloride (2.6 mmol) was added dropwise to the reaction mixture at 0 °C. After stirring overnight, the reaction extracted with water and washed with brine. Organic phase dried over magnesium sulfate and evaporated. The residue was purified with flash chromatography using an ethyl acetate:DCM (30:70) solvent system to give the desired product.

(*S*)-Glycidyl *N*-Methylsulfonyl-4-aminophenyl Ether (15)

White solid (70% yield). ^{1}H NMR (400 MHz, $CDCl_3$) δ 2.77 (1H, dd, J = 2.4, 5.2 Hz), 2.92 (1H, t, J = 4.4 Hz), 2.95 (3H, s), 3.34–3.36 (1H, m), 3.92 (1H, dd, J = 5.6, 11.2 Hz), 4.24 (1H, dd, J = 2.8, 11.2 Hz), 6.34 (1H, s), 6.91 (2H, dd, J = 2.0, 6.9 Hz), 7.19 (2H, dd, J = 2.0,

6.9 Hz). ^{13}C NMR (100 MHz, $CDCl_3$) δ 39.197, 44.839, 50.305, 69.298, 115.850, 124.814, 129.770, 157.182. MS (FAB): 243.00, calcd 243.06

General Method For Preparation of (*S*)-Glycidyl *N*-Substituted Acetamidophenyl Ether

(*S*)-Glycidyl 4-aminophenyl ether (2.4 mmol) dissolved in 20 mL anhydrous DCM and *N*,*N*-diisopropyl-*N*-ethylamine (2.6 mmol) was added at 0 °C. After stirring 15 min, substituted acetyl chloride (2.6 mmol) was added dropwise to the reaction mixture at 0 °C. After stirring overnight, the reaction extracted with water and washed with brine. Organic phase dried over magnesium sulfate and evaporated. The residue was purified with flash chromatography using an ethyl acetate:DCM (30:70) solvent system to give the desired product.

(*S*)-Glycidyl *N*-acetamidophenyl Ether (25)

White solid, 59% yield. ^{1}H NMR (400 MHz, $CDCl_3$) δ 2.13 (3H, s), 2.74 (1H, dd, *J* = 3.2, 4.8 Hz), 2.90 (1H, t, *J* = 4.8 Hz), 3.32–3.35 (1H, m), 3.90 (1H, dd, *J* = 5.6, 11.2 Hz), 4.19 (1H, dd, *J* = 3.2, 11.2 Hz), 6.85 (2H, dd, *J* = 2.4, 6.8 Hz), 7.38 (2H, dd, *J* = 2.4, 6.8 Hz), 7.46 (1H, brs). ^{13}C NMR (100 MHz, $CDCl_3$) δ 24.49, 44.87, 50.37, 69.21, 115.11, 122.03, 131.75, 155.42, 168.58

General Method for Synthesizing Compounds 29–43

Appropriate aminophenylether (2.00 mmol) and 3,4-dichlorophenylethylamine (2.00 mmol) were heated under reflux conditions in 20 mL ethanol for 4–24 h. Then solvent was evaporated and residue was purified with flash chromatography using a dichloromethane: methanol (90:10) solvent system.

(*S*)-1-(4-Methanesulfonamidephenoxy)-3-(3,4-dichlorophenylethylamino)-2-propanol (29)

Colorless oil, 80% yield; $[\alpha]_D^{20} = -12.6$. ^{1}H NMR (400 MHz, $CDCl_3$) δ 2.75–2.93 (6H, m), 2.95 (3H, s), 3.94, (1H, d, Hα, *J* = 2.4 Hz), 3.96 (1H, s, H*β*), 4.00–4.05 (1H, m), 6.88 (2H, dd, *J* = 2.0, 6.8 Hz), 7.04 (1H, dd, *J* = 2.4, 8.0 Hz), 7.18 (2H, dd, *J* = 2.4, 6.8 Hz), 7.30 (1H, d, *J* = 2.0 Hz), 7.35 (1H, d, *J* = 8.4 Hz). ^{13}C NMR (100 MHz, $CDCl_3$) δ 35.82, 39.24, 50.71, 51.65, 68.34, 70.91, 115.69, 124.97, 128.39, 129.55, 130, 52, 130.63, 130.86, 140.27, 157.36. Compound **29** was dissolved in ethanol and bubbled HCl gas to get the HCl salt of the compound **29** as a white solid. MS (FAB): 469.5954, calcd 469.81. Anal. ($C_{18}H_{23}Cl_3N_2O_4S$)C, H, N.

2-Phenyl-3-(*N*-3,4-dichlorophenylethylamino)-5-(2-nitrophe-noxy methyl)oxazolidine (45)

Compound **44** (2.6 mmol), benzaldehyde (2.96 mmol), and *p*-toluenesulfonic acid (catalytic amount) were dissolved in 50 mL of toluene and refluxed in a Dean–Stark apparatus for 30 h, cooled, and extracted with saturated sodium bicarbonate. The organic layer was dried over $MgSO_4$ and evaporated, yielding yellow oil. It was clean enough for the next step. There was no separation of the stereoisomer. ^{1}H NMR (400 MHz, CDCl3) δ 2.61–2.99 (10H, m), 3.56 (1H, dd, *J* = 2.4, 9.6 Hz), 3.61 (1H, dd, *J* = 2.4, 8.8 Hz), 3.83 (1H, t, *J* = 7.2 Hz), 4.03 (1H, t, *J* = 8.4 Hz), 4.20 (2H, dd, *J* = 4.4, 8.8 Hz), 4.32 (2H, dd, *J* = 4.0, 10.0 Hz), 4.54–4.58 (1H, m), 4.64–4.69 (1H, m), 4.81 (1H, s), 4.94 (1H, s), 6.88 (1H, dd, *J* = 2.0, 8.0 Hz), 6.93 (1H, dd, *J* = 2.0, 8.4 Hz), 7.04–7.21 (6H, m), 7.26–7.43 (12H, m), 7.51 (1H, d, *J* = 6.8 Hz), 7.55 (1H, d, *J* = 6.4 Hz), 7.85 (1H, dd, *J* = 2.0, 8.0 Hz), 7.88 (1H, dd, *J* = 2.4, 8.8 Hz).

2-Phenyl-3-(*N*-phenylethylamino)-5-(2-aminophenoxymethyl)oxazolidine (46)

Compound **45** (2.7 mmol) was dissolved in 30 mL of ethanol, 1.28 mL of 2N sodium hydroxide, and 0.128 g Pd/C (%10) (10% of the weight of starting material) was added to

the solution. The reaction was hydrogenated at ambient pressure and temperature for 12 h. The reaction mixture was filtered by using membrane filter (13, 0.22 μm), and the filtrate was concentrated in vacuum, leaving yellow oil. This oil was dissolved in DCM and extracted with water, dried over $MgSO_4$, and the solvent removed leaving colorless oil (39% yield). The amine was used directly in the next step without purification.

1-(2-Methanesulfonamidophenoxy)-3-(3,4-dichlorophenylethylamino)-2-propanol (43)

Compound **46** (1.05 mmol) was dissolved in DCM and cooled to 0 °C. At 0 °C, *N*,*N*-diisopropyl-*N*-ethylamine (1.15 mmol) and methane sulfonyl chloride (1.15 mmol) was added to the reaction. The reaction mixture was stirred at 0 °C for 2 h, then warmed to room temperature slowly and stirred at room temperature for another 16 h. Solvent was evaporated, leaving a yellow-brown oil. The latter was added to 50 mL of 1N HCl solution and stirred at room temperature for 4 h and extracted with DCM. The water layer was removed under reduced pressure, and the resulting solid was recrystallized from ethanol/ether to give the hydrochloride salt of compound **43** (white solid, 43% yield). ^{1}H NMR (400 MHz, DMSO-d_6) δ 2.34 (3H, s), 2.93–3.39 (6H, m), 3.94–4.10 (2H, m), 4.15–4.30 (1H, m), 6.55–7.03 (2H, m), 7.24–7.60 (5H, m), 8.74 (1H, s). ^{13}C-NMR (100 MHz, DMSO-d_6) δ 39.56, 40.87, 50.99, 51.56, 58.59, 69.88, 114.97, 126.43, 130.26, 130.58, 138, 79, 150.22, 150.98, 158.75, 165.48. Anal. ($C_{18}H_{23}Cl_3N_2O_4S$) C, H, N.

General Method for compound 47–65

First, 1.5 mmol of (*S*)-glycidyl *N*-substituted-4-aminophenyl ether (**15–28**) and 1.5 mmol of suitable phenyl ethylamine were dissolved in 5 mL of ethanol and refluxed for 6–24 h. After refluxing time, the solvent evaporated and the residue was purified by flash chromatography using a dichloromethane:methanol (90:10) solvent system to give the products as colorless oil (40–90% yield).

(*S*)-1-(4-Methanesulfonamidophenoxy)-3-(2-chlorophenylethylamino)-2-propanol (47)

Yield 62%. ^{1}H NMR (400 MHz, DMSO-d_6) δ 2.54–2.79 (6H, m), 2.83 (3H, s), 3.76–3.88 (3H, m), 4.92 (1H, brs), 6.87 (2H, d, J = 9.0 Hz), 7.09 (2H, d, J = 9.0 Hz), 7.19 (2H, dd, J = 3.3, 6.3 Hz), 7.33 (2H, dt, J = 2.4 8.7 Hz). Anal. ($C_{18}H_{24}Cl_zN_2O_4S$) C, H, N.

General Method for compound 67–102

One mmol of compound **29** and 1 mmol of appropriate aldehyde were dissolved in 10 mL of 1,2-dichloroethane and treated with 1.4 mmol of sodium triacetoxyborohydride. After stirring overnight at room temperature, the reaction mixture was quenched with saturated sodium bicarbonate. Water phase was extracted with 1,2-dichloroethane. Organic phase dried over $MgSO_4$ and evaporated. The residue was purified with flash chromatography to give a colorless oil.

(*S*)-1-(4-Methanesulfonamidophenoxy)-3-(*N*-ethyl-3,4-dichlorophenylethylamino)-2-propanol (67)

Yield 72%, solvent system for flash chromatography DCM:MeOH (90:10). ^{1}H NMR (400 MHz, $CDCl_3$) δ 1.03 (3H, t, J = 7.2 Hz), 2.58–2.80 (8H, m), 2.91 (3H, s), 3.88, (1H, d, Hα, J = 4.8 Hz), 3.90 (1H, s, Hβ), 3.94–3.96 (1H, m), 6.83 (2H, dd, J = 2.4, 6.8 Hz), 6.99 (1H, dd, J = 2.0, 8.4 Hz), 7.16 (2H, dd, J = 2.0, 7.2 Hz), 7.25 (1H, d, J = 2.0 Hz), 7.31 (1H, d, J = 8.0 Hz). ^{13}C NMR (100 MHz, $CDCl_3$) δ 15.16, 33.11, 42.24, 48.56, 59.29, 60.12, 66.30, 70.65, 116.59, 125.06, 128.57, 129.54, 130.38, 130.75, 130.96, 141.23, 157.56. Compound **67** was dissolved in ethanol and bubbled HCl gas to get the HCl salt of the compound **67**. Anal. ($C_{20}H_{27}Cl_3N_2O_4S$) C, H, N.

Molecular Modeling

Seven molecular structures (**29**, **30**, **52**, **67**, **91**, **103**, and ifenprodil) were geometry optimized with the MMFF force field[69–73] and then subjected to a conformational search using OMEGA.[42] Care was taken to ensure identical chirality and protonation states for all molecules. Certain default parameters were changed (ewindow 25.0, maxconfgen 100000, maxconfs 1000, maxtime 75.0, rms 0.5, enumNitrogen false) to ensure a more complete conformer pool for subsequent analysis. The resulting combined libraries of conformers (1000 conformers for the propanolamine structures, 75 for ifenprodil) was then searched using ROCS,[43] which provides a rapid comparison of 3D molecular shape to a query structure. The query structure was taken from an MMFF-optimized pose of **67** docked to a homology model of the NR2B ATD subunit.[47] The 75 most shape-congruent structures from ROCS were then analyzed in a second step using the program EON.[44] The latter gauges the molecular similarity of two structures by comparing electrostatic potentials of the molecules in question. The top scoring conformer from the EON analysis was kept as the best match, both in shape and electrostatic nature, to the query structure. These conformers are shown in Figures 3 and 4, and their similarity scores presented in Table 6.

Expression of Glutamate Receptors in *Xenopus laevis* Oocytes

All protocols involving the use of animals were approved by the Emory University or Duke University IACUC. cRNA was synthesized from linearized template cDNA for rat glutamate receptor subunits according to manufacturer specifications (Ambion). Quality of synthesized cRNA was assessed by gel electrophoresis, and quantity was estimated by spectroscopy and gel electrophoresis. Stage V and VI oocytes were surgically removed from the ovaries of large, well-fed, and healthy *Xenopus laevis* anesthetized with 3-amino-benzoic acid ethyl ester (3 g/L) as previously described.[74] Clusters of isolated oocytes were incubated with 292 U/mL Worthington (Freehold, NJ) type IV collagenase or 1.3 mg/mL collagenase (Life Technologies, Gaithersburg, MD; 17018-029) for 2 h in Ca^{2+}-free solution composed of (in mM) 115 NaCl, 2.5 KCl, and 10 HEPES, pH 7.5, with slow agitation to remove the follicular cell layer. Oocytes were then washed extensively in the same solution supplemented with 1.8 mM $CaCl_2$ and maintained in Barth's solution composed of (in mM): 88 NaCl, 1 KCl, 2.4 $NaHCO_3$, 10 HEPES, 0.82 $MgSO_4$, 0.33 $Ca(NO_3)_2$, and 0.91 $CaCl_2$ and supplemented with 100 μg/mL of gentamycin, 10 μg/mL of streptomycin, and 10 μg/mL of penicillin. Oocytes were manually defolliculated and injected within 24 h of isolation with 3–5 ng of NR1 subunit and 7–10 ng of NR2 subunit in a 50 nL volume, or 5–10 ng in 50 nL of AMPA or kainate receptor cRNAs, and incubated in Barth's solution at 18 °C for 1–7 d. Glass injection pipettes had tip sizes ranging from 10–20 μm and were backfilled with mineral oil.

Two Electrode Voltage Clamp Recording from *Xenopus laevis* Oocytes

Two electrode voltage-clamp recordings were made 2–7 days postinjection as previously described.[74] Oocytes were placed in a dual-track plexiglass recording chamber with a single perfusion line that splits in a Y-configuration to perfuse two oocytes. Dual recordings were made at room temperature (23 °C) using two Warner OC725B two-electrode voltage clamp amplifiers, arranged as recommended by the manufacturer. Glass microelectrodes (1–10 megaohms) were filled with 300 mM KCl (voltage electrode) or 3 M KCl (current electrode). The bath clamps communicated across silver chloride wires placed into each side of the recording chamber, both of which were assumed to be at a reference potential of 0 mV. Oocytes were perfused with a solution comprised of (in mM) 90 NaCl, 1 KCl, 10 HEPES, and 0.5 $BaCl_2$; pH was adjusted to 7.3 or 7.6 by addition of 1–3 M NaOH. Oocytes were recorded under voltage clamp at −40 mV. Final concentrations for control application of glutamate (50 μM) plus glycine (30 μM) were achieved by adding appropriate volumes from 100 and 30 mM stock solutions, respectively. In addition, 10 μM final EDTA was

obtained by adding a 1:1000 dilution of 10 mM EDTA in order to chelate contaminant divalent ions such as Zn^{2+}. Concentration–response curves for experimental compounds were obtained by applying in successive fashion maximal glutamate/glycine, followed by glutamate/glycine plus variable concentrations of experimental compounds. Dose response curves consisting of 4–8 concentrations were obtained in this manner. The baseline leak current at −40 mV was measured before and after recording, and the full recording linearly corrected for any change in leak current. Oocytes with glutamate-evoked responses smaller than 50 nA were not included in the analysis. The level of inhibition by applied experimental compounds was expressed as a percent of the initial glutamate response and averaged together across oocytes from a single frog. Each experiment consisted of recordings from 3 to 10 oocytes obtained from a single frog. Results from 3–6 experiments were pooled, and the percent responses at antagonist concentrations for each oocyte were fitted by the equation,

$$\text{Percent Response} = (100 - \text{minimum}) / (1 + ([\text{conc}] / \text{IC}_{50})\, nH) + \text{minimum}$$

where minimum is the residual percent response in saturating concentration of the experimental compounds, IC_{50} is the concentration of antagonist that causes half of the achievable inhibition, and *nH* is a slope factor describing steepness of the inhibition curve. Minimum was constrained to be greater than or equal to 0.

Whole Cell Patch Clamp Recording of Voltage-Activated Currents in Neurons

Neuronal cultures were derived from E17 Sprague–Dawley rat pups. Briefly, cortical tissue was dissected, transferred into saline containing penicillin/streptomycin and 10 mM HEPES, and incubated in trypsin containing 0.02% DNase at 37 °C for 15 min. Tissue was then triturated and the supernatant resuspended in B27-supplemented Neurobasal media (Gibco) containing 2 mM L-glutamine and 5% fetal bovine serum. Cells were plated onto poly-D-lysine-coated coverslips, and after three days, the media was replaced with serum-free media. Cultures were maintained at 37 °C in a humidified 5% CO_2-containing atmosphere. Whole-cell patch clamp recordings (voltage clamp, holding potential −60 mV) from 5- to 10-day cultured cortical neurons were made with an Axopatch 200B amplifier (Axon Instruments, Union City, CA) at room temperature (23 °C). The recording chamber was continually perfused with recording solution composed of (in mM) 150 NaCl, 3 KCl, 2 $CaCl_2$, 1.5 $MgCl_2$, 5.5 glucose, and 10 HEPES (pH 7.4 by NaOH; osmolality adjusted to 315 mOsm with sucrose). Thin wall glass pipettes were filled with (in mM) 110 D-gluconate (50% w/w), 110 CsOH (50% w/w), 30 CsCl, 5 HEPES, 4 NaCl, 0.5 $CaCl_2$, 2 $MgCl_2$, 5 BAPTA, 2 NaATP, and 0.3 NaGTP (pH adjusted to 7.3 with CsOH and osmolality adjusted to 300 mOsm with sucrose). Recordings were made in the presence of 10 μM bicuculline, 10 μM CNQX, and 100 μM DL-APV to block both excitatory and inhibitory synaptic transmission. Drugs were applied by gravity and controlled by manual valves. Voltage-gated macroscopic whole cell currents were activated by 100 ms voltage steps from a holding potential of −60 mV to between −90 and +50 mV. The sensitivity of Na^+ currents to 0.5 μM tetrodotoxin was confirmed at the end of each experiment; K^+ channels were recorded in the presence of 0.5 μM tetrodotoxin to block Na^+ channels. We evaluated the mean Na^+ current from a number of whole cell recordings at −10 mV, and the mean K^+ current at +50 mV using a paired *t* test.

In Vitro Assay of Neuronal Death

Primary dissociated cortical cultures were prepared from Sprague–Dawley rat embryos (E16-E19) as previously described.[19] After 9–12 days in culture, pretreatment and treatment

of cells with experimental compounds were performed using buffered artificial cerebrospinal fluid (ACSF) solution (pH 7.6). ACSF was comprised of (in mM) 130 NaCl, 3.5 KCl, 2 $MgSO_4$, 1.25 NaH_2PO_4, 2 $CaCl_2$, 15 $NaHCO_3$, 10 glucose, and 10 HEPES and saturated with 95%O_2/5% CO_2. Cells were pretreated with ACSF alone, variable concentrations of test compound, or D-APV (100 μM) for 15 min. Excitotoxicity was induced by treating cultures with NMDA (100 μM) plus glycine (10 μM) at room temperature for 10 min in the presence of test compound or D-APV (100 μM). Cells were subsequently washed twice with fresh medium containing D-APV (100 μM) and CNQX (1–10 μM) to limit the period of excitotoxicity to the 10 min exposure. Rinsed plates were returned to the incubator in fresh medium without D-APV or CNQX. After 16–24 h, excitotoxic damage was assessed spectrophotometrically measuring the amount of lactate dehydrogenase (LDH) released into the culture medium (Tox-7 kit; Sigma Chemical Co, St. Louis, MO). Released LDH was expressed as the fraction of total LDH present in each well, determined by lysing the cells. Neuroprotection produced by experimental compounds was quantified by scaling LDH release in wells between minimum and maximum degree of LDH release. We defined percent inhibition as

$$\%\text{Inhibition} = 100 - 100\,(\text{LDHtreated} - \text{LDHmin}) / (\text{LDHmax} - \text{LDHmin})$$

where LDHtreated is the amount of LDH released from wells treated with variable concentrations of experimental compound **29**, LDH-min was the LDH release from wells treated with ACSF+D-APV, and LDHmax was the maximum LDH released from wells treated with glutamate and glycine. Cultures in which the NMDA-evoked excitotoxic cell death was less than 10% were discarded.

Transient Focal Ischemia

Transient focal cerebral ischemia was induced in mice by intraluminal middle cerebral artery occlusion (MCAO) with a monofilament suture as previously described.[75] Male C57BL/6 mice (3–5 months old, The Jackson Laboratory) were anesthetized with 2% isoflurane in 98% O_2. The rectal temperature was controlled at 37 °C (range 36.5–37.5) with a homeothermic blanket. Relative changes in regional cerebral blood flow were monitored with a laser Doppler flowmeter (Perimed). To do this, the probe was glued directly to the skull 2 mm posterior and 4–6 mm lateral of the bregma. An 11 mm 5–0 Dermalon or Look (SP185) black nylon nonabsorbable suture with the tip flame-rounded was introduced into the left internal carotid artery through the external carotid artery stump until monitored blood flow was reduced below 20% or stopped (at 10.5–11 mm of suture insertion). After 30 min MCA occlusion, blood flow was restored by withdrawing the suture. After 24 h survival, the brain was removed and cut into 2 mm sections. The lesion was identified with 2% 2,3,5-triphenyltetrazolium chloride (TTC) in PBS at 37 °C for 20 min. The infarct area of each section was measured using NIH IMAGE (Scion Corporation, Beta 4.0.2 release) and multiplied by the section thickness to give the infarct volume of that section. The density slice option in NIH IMAGE was used to segment the images based on the intensity determined as 70% of that in the contralateral undamaged cortex. This standard was maintained throughout the analysis in all animals, and only objects at this intensity were highlighted for area measurement. The area of the lesion, as identified by digital threshold reductions in TTC staining, was manually outlined. A ratio of the contralateral to ipsilateral hemisphere section volume was multiplied by the corresponding infarct section volume to correct for edema. Infarct volume was determined by summing the infarct area times section thickness for all sections. C57Bl/6 mice received an intraperitoneal (ip) injection of compound **29** 10 min before MCA occlusion surgery, resulting in receipt of compound **29** 30 min before occlusion. A 30 mg/mL stock solution in 50% DMSO was prepared by

adding 30 mg of compound into 0.5 mL of DMSO followed by addition of 0.5 mL of 0.9% saline with vortexing. The working solution for the ip injection solution was 3 mg/mL in 0.9% saline (50% v/v DMSO) and was prepared by transferring 0.2 mL of the stock solution into a new tube and adding 0.9 mL of DMSO and 0.9 mL of 0.9% saline with vortexing. A dose of 30 mg/kg compound **29** was administered to mice with a 10 mL/kg injection volume. The technician performing both the surgical procedure and analysis of stained sections by NIH IMAGE was blinded from the compound injected.

Maximal Electroshock-Induced Seizures

One or two drops of 1% lidocaine were placed in each conjunctiva of 100–125 g male Sprague–Dawley rats (Zivic Miller). Approximately 30–60 s later, the animal was picked up gently, restrained gently, and a cup electrode was placed over each cornea and a constant current stimulus (200 mA, 60 Hz, 0.2 s) was administered (Wahlquist Instrument Co., Salt Lake City, UT). Seizure onset occurred virtually instantaneously with the onset of current flow. The duration of tonic hind limb flexion, tonic hind limb extension, and time to recovery were recorded. Measurements of these parameters were made on three sequential days. Untreated animals were tested on the first and third day. The second day tested the indicated amounts of experimental compounds administered ip in DMSO. Vehicle-injected animals served as negative controls, and carbamazepine treated animals (60 mg/kg) served as positive controls. The duration of tonic hind limb extension was visually scored, and the data were analyzed by ANOVA with Bonferroni's *t* test post hoc. Differences were considered significant if $p < 0.05$.

Locomotor Activity Testing

Locomotor activity was measured using eight Digiscan activity monitors (AccuScan Instruments, Inc., Columbus, OH) with the aid of the VersaMax software (Version 1.30, Omnitech Instruments Inc.).[76] Sprague–Dawley rats (100–200 g) were tested in a 40 cm × 40 cm × 30 cm (L × W × H) clear acrylic chamber surrounded by a framework of infrared photobeams. Each chamber was individually housed in a ventilated, sound-attenuating cubicle that was illuminated by incandescent light (approximately 45 l×). The infrared photobeams were in a 16 × 16 array around the bottom of the box and 2.5 cm from the floor. Movements were determined by breaks in photobeams and were converted into locomotor activity counts with the aid of VersaDat software (Version 1.3; AccuScan Instruments Inc.), which was interfaced with a microcomputer.

On testing days, animals were taken from the colony room and moved to the testing room in their home cages. Animals were habituated to the testing room for at least 30 min before they were placed in activity chambers. Basal activity was measured for 1 h in the activity box. Animals were subsequently removed and injected with appropriate dose of test agent ip and returned to the activity box for 2 h. Compounds were formulated either in sterile 0.9% saline (selfotel and aptiganel), 5% (2-hydroxypropyl)-β-cylodextrin in H_2O (ifenprodil), or 10% DMSO in PEG **(111** (Figure 1)). Propanolamine **29** was delivered in either 10% DMSO in PEG or 50% DMSO in saline. When DMSO was used for formulation, the compound was first dissolved in DMSO and then diluted to the desired final concentration with PEG or saline, with vortexing. We analyzed horizontal activity counts (ambulation) and expressed the measurements as number of photobeam breaks. Vehicle injected animals were run each day as negative control animals, and 0.3 mg/kg **110,** ip in saline, which strongly stimulates locomotor activity, was used as a positive control each day. A strong locomotor response to **110** was observed (38233 ± 7213 counts, $n = 11$) without exception in all animals on all testing days.

Rotorod

Mice were tested in the rotorod assay, a well recognized test for sensorimotor function, using a four-chamber Rotamex 4/8 rotorod (Columbus Instruments, Columbus, OH). The test is initiated by placing mice on a rotating rod (5 rpm) that was 3.8 cm diameter by 8 cm wide and suspended 30 cm from the floor of a chamber. After 10 s, the rotation is accelerated from 5 to 35 rpm over a 5 min period. The time the mouse falls from the rod (the latency time) is recorded automatically with a light-activated sensor in the bottom of the chamber. Animals were tested four times each day for five days, with a within-day intertrial interval of 25 min and a between-day interval of 24 h. On day 5, mice were randomly assigned to three groups and injected ip with either vehicle, 0.3 mg/kg **110,** or 30 mg/kg propanolamine **29**. Drugs were dissolved in 25% DMSO, 75% saline and injected in a 5 mL/kg volume. The technician conducting the rotorod assay was blinded.

Plasma Half-Life and Brain Exposure of Propanolamines

Rats (n = 3 per dose) were administered compounds at a dose of 4 mg/kg in a single bolus iv infusion (2 mL/kg body weight) via the tail vein, or 30 mg/kg ip, formulated in 2% dimethyl acetamide/98% 2-hydroxy-propyl cyclodextrin (5%). For the plasma stability studies, the test article was prepared in 50% DMSO/50% water such that the final solvent concentration in plasma did not exceed 0.5% (v/v).

Animals were fasted overnight prior to dose administration and food returned to the animals two hours after dosing. Following iv dosing, blood samples (ca. 200 μL) were collected into separate tubes containing anticoagulant (K-EDTA) via the orbital plexus at 5, 30, 120, and 240 min. Plasma samples were prepared immediately after collection by centrifugation for 10 min using a tabletop centrifuge, and the plasma stored at <−20 °C. Brain tissue was weighed, homogenized on ice in 50 mM phosphate buffer (2 mL per brain) and the homogenate was stored at <−20 °C. Plasma and brain homogenate samples were extracted by the addition of 5 volumes of cold acetonitrile, mixed well by vortexing, and centrifuged at 4000 rpm for 15 min. The supernatant fractions were analyzed by LC-MS/MS operating in multiple reaction monitoring mode (MRM). The amount of parent compound in each sample was calculated by comparing the response of the analyte in the sample to that of a standard curve. Analysis of samples was performed by Ricerca Biosciences, LLC (Concord, OH).

In Vitro Binding Studies

Compounds in Table 7 were evaluated for binding to the human ether-a-go-go potassium channel (hERG) expressed in HEK293 cells by displacement of ^{3}[H]-astemizole[78] Binding to the rat α-1 adrenergic receptor in rat brain membranes was determined by displacement of ^{3}[H]-prazosin.[79] Binding IC_{50} values were determined from displacement curves (4–6 concentrations, each point in duplicate) fit by a nonlinear, least-squares, regression analysis using MathIQ (ID Business Solutions Ltd., UK).

Supplementary Material

Refer to Web version on PubMed Central for supplementary material.

Acknowledgments

We thank Drs. Elias Aizenman, Stephen Heinemann, Shigetada Nakanishi, Pierre Paoletti, and Peter Seeburg for sharing cDNA for glutamate receptors and mutants, and Dr. Mark Washburn for assistance in several of the biological assays. We are also grateful to OpenEye Scientific Software (Santa Fe, NM) for the generous provision of a no-cost license to use software for the conformational analyses described. This work was supported by NIH-NINDS (NS036654, NS039419 S.T.), NARSAD (S.T.), NIH-NINDS (NS036604, R.D.), NIH-NINDS NS056217

(J.O.M.), the Michael J. Fox Foundation (S.T.), and Parents Against Childhood Epilepsy, Inc. Research Grant Program (R.D.).

References

1. Dingledine R, Borges K, Bowie D, Traynelis SF. The glutamate receptor ion channels. Pharmacol Rev. 1999; 51:7–61. [PubMed: 10049997]
2. Erreger K, Chen P, Wyllie DJA, SF T. Glutamate receptor gating. Crit Rev Neurobiol. 2004; 16:187–224. [PubMed: 15701057]
3. Kew JNC, Kemp JA. Ionotropic and metabotropic glutamate receptor structure and pharmacology. Psychopharmacology. 2005; 179:4–29. [PubMed: 15731895]
4. Chenard BL, Menniti FS. Antagonists selective for NMDA receptors containing the NR2B subunit. Curr Pharm Des. 1999; 5:381–404. [PubMed: 10213801]
5. Chazot PL. The NMDA receptor NR2B subunit: a valid therapeutic target for multiple CNS pathologies. Curr Med Chem. 2004; 11:389–396. [PubMed: 14965239]
6. Wang C, Shuaib A. NMDA/NR2B selective antagonists in the treatment of ischemic brain injury. Curr Drug Targets CNS Neurol Disord. 2005; 4:143–151. [PubMed: 15857299]
7. Layton ME, Kelly MJ, Rodzinak KJ. Recent advances in the development of NR2B subtype-selective NMDA receptor antagonists. Curr Top Med Chem. 2006; 6:697–709. [PubMed: 16719810]
8. Moriyoshi K, Masu M, Ishii T, Shigemoto R, Mizuno N, Nakanishi S. Molecular-Cloning and Characterization of the Rat NMDA Receptor. Nature. 1991; 354:31–37. [PubMed: 1834949]
9. Sugihara H, Moriyoshi K, Ishii T, Masu M, Nakanishi S. Structures and Properties of 7 Isoforms of the NMDA Receptor Generated by Alternative Splicing. Biochem Biophys Res Commun. 1992; 185:826–832. [PubMed: 1352681]
10. Monyer H, Sprengel R, Schoepfer R, Herb A, Higuchi M, Lomeli H, Burnashev N, Sakmann B, Seeburg PH. Heteromeric NMDA Receptors: Molecular and Functional Distinction of Subtypes. Science. 1992; 256:1217–1221. [PubMed: 1350383]
11. Monyer H, Burnashev N, Laurie DJ, Sakmann B, Seeburg PH. Developmental and Regional Expression in the Rat-Brain and Functional Properties of 4 NMDA Receptors. Neuron. 1994; 12:529–540. [PubMed: 7512349]
12. Choi YB, Lipton SA. Identification and mechanism of action of two histidine residues underlying high-affinity Zn^{2+} inhibition of the NMDA receptor. Neuron. 1999; 23:171–180. [PubMed: 10402203]
13. Low CM, Zheng F, Lyuboslavsky P, Traynelis SF. Molecular determinants of coordinated proton and zinc inhibition of *N*-methyl-d-aspartate NR1/NR2A receptors. Proc Natl Acad Sci U S A. 2000; 97:11062–11067. [PubMed: 10984504]
14. Paoletti P, P-D F, Fayyazuddin A, Le Goff A, Callebaut I, Neyton J. Molecular organization of zinc binding N-terminal modulatory domain in a NMDA receptor subunit. Neuron. 2000; 28:911–925. [PubMed: 11163276]
15. Perin-Dureau F, Rachline J, Neyton J, Paoletti P. Mapping the binding site of the neuroprotectant ifenprodil on NMDA receptors. J Neurosci. 2002; 22:5955–5965. [PubMed: 12122058]
16. Williams K. Ifenprodil Discriminates Subtypes of the *N*-Methyl-d-Aspartate Receptor: Selectivity and Mechanisms at Recombinant Heteromeric Receptors. Mol Pharmacol. 1993; 44:851–859. [PubMed: 7901753]
17. Scatton, B.; Avenet, P.; Benavides, J.; Carter, C.; Duverger, D.; Oblin, A.; Perrault, G.; Sanger, DJ.; Schoemaker, H. Neuroprotective Potential of the Polyamine site-directed NMDA Receptor Antagonists: Ifenprodil and Eliprodil. In: Palfreyman, MG.; Reynolds, IJ.; Skolnick, P., editors. Direct and Allosteric Control of Glutamate Receptors. CRC Press; Boca Raton, FL: 1994. p. 139
18. Chenard BL, Bordner J, Butler TW, Chambers LK, Collins MA, Decosta DL, Ducat MF, Dumont ML, Fox CB, Mena EE, Menniti FS, Nielsen J, Pagnozzi MJ, Richter KEG, Ronau RT, Shalaby IA, Stemple JZ, White WF. (1*S*,2*S*)-1-(4-Hydroxyphenyl)-2-(4-Hydroxy-4-Phenylpiperidino)-1-Propanol: A Potent New Neuroprotectant Which Blocks *N*-Methyl-d-Aspartate Responses. J Med Chem. 1995; 38:3138–3145. [PubMed: 7636876]

19. Mott DD, Doherty JJ, Zhang SN, Washburn MS, Fendley MJ, Lyuboslavsky P, Traynelis SF, Dingledine R. Phenyletha-nolamines inhibit NMDA receptors by enhancing proton inhibition. Nat Neurosci. 1998; 1:659–667. [PubMed: 10196581]
20. Fischer G, Mutel V, Trube G, Malherbe P, Kew JNC, Mohacsi E, Heitz MP, Kemp JA. Ro 25-6981, a highly potent and selective blocker of *N*-methyl-d-aspartate receptors containing the NR2B subunit. Characterization in vitro. J Pharmacol Exp Ther. 1997; 283:1285–1292. [PubMed: 9400004]
21. Barta-Szalai G, Borza I, Bozo E, Kiss C, Agai B, Proszenyak A, Keseru GM, Gere A, Kolok S, Galgoczy K, Horvath C, Farkas S, Domany G. Oxamides as novel NR2B selective NMDA receptor antagonists. Bioorg Med Chem Lett. 2004; 14:3953–3956. [PubMed: 15225705]
22. McCauley JA, Theberge CR, Romano JJ, Billings SB, Anderson KD, Claremon DA, Freidinger RM, Bednar RA, Mosser SD, Gaul SL, Connolly TM, Condra CL, Xia MH, Cunningham ME, Bednar B, Stump GL, Lynch JJ, Macaulay A, Wafford KA, Koblan KS, Liverton NJ. NR2B-selective *N*-methyl-d-aspartate antagonists: synthesis and evaluation of 5-substituted benzimidazoles. J Med Chem. 2004; 47:2089–2096. [PubMed: 15056006]
23. Borza I, Kolok S, Gere A, Agai-Csongor E, Agai B, Tarkanyi G, Horvath C, Barta-Szalai G, Bozo E, Kiss C, Bielik A, Nagy J, Farkas S, Domany G. Indole-2-carboxamides as novel NR2B selective NMDA receptor antagonists. Bioorg Med Chem Lett. 2003; 13:3859–3861. [PubMed: 14552795]
24. Curtis NR, Diggle HJ, Kulagowski JJ, London C, Grimwood S, Hutson PH, Murray F, Richards P, Macaulay A, Wafford KA. Novel *N*-1-(benzyl)cinnamamidine derived NR2B subtype-selective NMDA receptor antagonists. Bioorg Med Chem Lett. 2003; 13:693–696. [PubMed: 12639560]
25. Wright, JL.; Kesten, SR.; Upasani, RB.; LanN, C. 4-Benzylpip-eridinylalkylsulfinyl-substituted heterocycles and their use as subtype-selective NMDA receptor antagonists. WO 2000000197. 2000.
26. Tamiz AP, Cai SX, Zhou ZL, Yuen PW, Schelkun RM, Whittemore ER, Weber E, Woodward RM, Keana JFW. Structure–activity relationship of *N*-(phenylalkyl)cinnamides as novel NR2B subtype-selective NMDA receptor antagonists. J Med Chem. 1999; 42:3412–3420. [PubMed: 10464027]
27. Kitaori K, Furukawa Y, Yoshimoto H, Otera J. CsF in organic synthesis. Regioselective nucleophilic reactions of phenols with oxiranes leading to enantiopure beta-blockers. Tetrahedron. 1999; 55:14381–14390.
28. Sajiki H, Hattori K, Hirota K. The formation of a novel Pd/C-ethylenediamine complex catalyst: chemoselective hydrogenation without deprotection of the *O*-benzyl and *N*-Cbz groups. J Org Chem. 1998; 63:7990–7992.
29. Sajiki H, Hattori K, Hirota K. Highly chemoselective hydrogenation with retention of the epoxide function using a heterogeneous Pd/C: ethylenediamine catalyst and THF. Chem–Eur J. 2000; 6:2200–2204.
30. Choi WB, Wilson LJ, Yeola S, Liotta DC, Schinazi RF. In Situ Complexation Directs the Stereochemistry of *N*-Glycosylation in the Synthesis of Oxathiolanyl and Dioxolanyl Nucleoside Analogs. J Am Chem Soc. 1991; 113:9377–9379.
31. Connors SP, Gill EW, Terrar DA. Actions and Mechanisms of Action of Novel Analogs of Sotalol on Guinea Pig and Rabbit Ventricular Cells. Br j Pharmacol. 1992; 106:958–965. [PubMed: 1393293]
32. Ilyin VI, Whittemore ER, Guastella J, Weber E, Woodward RM. Subtype-selective inhibition of *N*-methyl-d-aspartate receptors by haloperidol. Mol Pharmacol. 1996; 50:1541–1550. [PubMed: 8967976]
33. Kew JN, Trube G, Kemp JA. A novel mechanism of activity-dependent NMDA receptor antagonism describes the effect of ifenprodil in rat cultured cortical neurones. J Physiol (London). 1996; 497:761–772. [PubMed: 9003561]
34. Kew JNC, Trube G, Kemp JA. State-dependent NMDA receptor antagonism by Ro 8-4304, a novel NR2B selective, non-competitive, voltage-independent antagonist. Br J Pharmacol. 1998; 123:463–472. [PubMed: 9504387]

35. Masuko T, Kashiwagi K, Kuno T, Nguyen ND, Pahk AJ, Fukuchi J, Igarashi K, Williams K. A regulatory domain (R1-R2) in the amino terminus of the *N*-methyl-d-aspartate receptor: Effects of spermine, protons, and ifenprodil, and structural similarity to bacterial leucine/isoleucine/valine binding protein. Mol Pharmacol. 1999; 55:957–969. [PubMed: 10347236]
36. Gallagher MJ, Huang H, Lynch DR. Modulation of the *N*-methyl-d-aspartate receptor by haloperidol: NR2B-specific interactions. J Neurochem. 1998; 70:2120–2128. [PubMed: 9572299]
37. Wong E, Ng FM, Yu CY, Lim P, Lim LH, Traynelis SF, Low CM. Expression and characterization of soluble amino-terminal domain of NR2B subunit of *N*-methyl-d-aspartate receptor. Protein Sci. 2005; 14:2275–2283. [PubMed: 16131656]
38. Rachline J, Perin-Dureau F, Le Goff A, Neyton J, Paoletti P. The micromolar zinc-binding domain on the NMDA receptor subunit NR2B. J Neurosci. 2005; 25:308–317. [PubMed: 15647474]
39. Pfeiffer CC. Optical Isomerism and Pharmacological Action, a Generalization. Science. 1956; 124:29–31. [PubMed: 13337345]
40. Mesecar AD, Koshland DE. A new model for protein stereospecificity. Nature. 2000; 408:668.
41. Mezzetti A, Schrag JD, Cheong CS, Kazlauskas RJ. Mirror-image packing in enantiomer discrimination: Molecular basis for the enantioselectivity of B-cepacia lipase toward 2-methyl-3-phenyl-1-propanol. Chem Biol. 2005; 12:427–437. [PubMed: 15850979]
42. Omega, version 2.0. Openeye Scientific Software, Inc; Santa Fe, NM: 2006.
43. Hawkins PCD, Skillman AG, Nicholls A. Comparison of Shape-Matching and Docking as virtual Screening Tools. J Med Chem. 2007; 50:74–82. [PubMed: 17201411]
44. EON, version 1.1. OpenEye Scientific Software, Inc; Santa Fe, NM: 2006.
45. Nicholls A, MacCuish NE, MacCuish JD. Variable Selection and Model Validation of 2D and 3D Molecular Descriptors. J Comput-Aided Mol Des. 2004; 18:451–474. [PubMed: 15729846]
46. Nicholls A, Grant JA. Molecular shape and electrostatics in the encoding of relevant chemical information. J Comput-Aided Mol Des. 2005; 19:661–686. [PubMed: 16328855]
47. Geballe, M.; Traynelis, S. F.; Snyder, J. P. unpublished.
48. McCauley JA, Theberge CR, Romano JJ, Billings SB, Anderson KD, Claremon DA, Freidinger RM, Bednar RA, Mosser SD, Gaul SL, Connolly TM, Condra CL, Xia MH, Cunningham ME, Bednar B, Stump GL, Lynch JJ, Macaulay A, Wafford KA, Koblan KS, Liverton NJ. NR2B-selective *N*-Methyl-d-aspartate antagonists: synthesis and evaluation of 5-substituted benzimidazoles. J Med Chem. 2004; 47:2089–2096. [PubMed: 15056006]
49. Whetsell WO. Current concepts of excitotoxicity. J Neuropath Exp Neur. 1996; 55:1–13. [PubMed: 8558164]
50. Dirnagl U, Iadecola C, Moskowitz MA. Pathobiology of ischaemic stroke: an integrated view. Trends Neurosci. 1999; 22:391–397. [PubMed: 10441299]
51. Brauner-Osborne H, Egebjerg J, Nielsen EO, Madsen U, Krogsgaard-Larsen P. Ligands for glutamate receptors: design and therapeutic prospects. J Med Chem. 2000; 43:2609–2645. [PubMed: 10893301]
52. Choi DW, Mauluccigedde M, Kriegstein AR. Glutamate Neurotoxicity in Cortical Cell Culture. J Neurosci. 1987; 7:357–368. [PubMed: 2880937]
53. Koh JY, Choi DW. Quantitative Determination of Glutamate Mediated Cortical Neuronal Injury in Cell Culture by Lactate-Dehydrogenase Efflux Assay. J Neurosci Methods. 1987; 20:83–90. [PubMed: 2884353]
54. Park CK, Nehls DG, Graham DI, Teasdale GM, Mcculloch J. The Glutamate Antagonist MK-801 Reduces Focal Ischemic Brain Damage in the Rat. Ann Neurol. 1988; 24:543–551. [PubMed: 2853604]
55. Miyabe M, Kirsch JR, Nishikawa T, Koehler RC, Traystman RJ. Comparative analysis of brain protection by *N*-methyl-d-aspartate receptor antagonists after transient focal ischemia in cats. Crit Care Med. 1997; 25:1037–1043. [PubMed: 9201058]
56. Dogan A, Rao AM, Baskaya MK, Rao VLR, Rastl J, Donaldson D, Dempsey RJ. Effects of ifenprodil, a polyamine site NMDA receptor antagonist on reperfusion injury after transient focal cerebral ischemia. J Neurosurg. 1997; 87:921–926. [PubMed: 9384405]

57. Bradford H. Glutamate, GABA, and epilepsy. Prog Neurobiol. 1995; 47:477–511. [PubMed: 8787032]
58. Kohl BK, Dannhardt G. The NMDA receptor complex: a promising target for novel antiepileptic strategies. Curr Med Chem. 2001; 8:1275–1289. [PubMed: 11562266]
59. Wlaz P, Ebert U, Loscher W. Anticonvulsant effects of eliprodil alone or combined with the glycine(B) receptor antagonist L-701324 or the competitive NMDA antagonist CGP 40116 in the amygdala kindling model in rats. Neuropharmacology. 1999; 38:243–251. [PubMed: 10218865]
60. Gill R, Alanine A, Bourson A, Buttelmann B, Fischer G, Heitz MP, Kew JNC, Levet-Trafit B, Lorez HP, Malherbe P, Miss MT, Mutel V, Pinard E, Roever S, Schmitt M, Trube G, Wybrecht R, Wyler R, Kemp JA. Pharmacological characterization of Ro 63-1908 (1-[2-(4-hydroxy-phenoxy)-ethyl]-4-(4-methyl-benzyl)-piperidin-4-ol), a novel subtype-selective *N*-methyl-d-aspartate antagonist. J Pharmacol Exp Ther. 2002; 302:940–948. [PubMed: 12183650]
61. McNamara, JO. Drugs Effective in the Therapies of the Epilepsies. 10th. McGraw Hill; New York: 2001. p. 521-547.
62. Ellison G. The *N*-Methyl-d-Aspartate Antagonists Phencyclidine, Ketamine and Dizocilpine as Both Behavioral and Anatomical Models of the Dementias. Brain Res Rev. 1995; 20:250–267. [PubMed: 7795658]
63. Thornberg SA, Saklad SR. Review of NMDA receptors and the phencyclidine model of schizophrenia. Pharmacotherapy. 1996; 16:82–93. [PubMed: 8700797]
64. Andine P, Widermark N, Axelsson R, Nyberg G, Olofsson U, Martensson E, Sandberg M. Characterization of MK-801-induced behavior as a putative rat model of psychosis. J Pharmacol Exp Ther. 1999; 290:1393–1408. [PubMed: 10454519]
65. Tricklebank MD, Singh L, Oles RJ, Preston C, Iversen SD. The Behavioral Effects of MK-801: A Comparison with Antagonists Acting Noncompetitively and Competitively at the NMDA Receptor. Eur J Pharmacol. 1989; 167:127–135. [PubMed: 2550253]
66. Hiramatsu M, Cho AK, Nabeshima T. Comparison of the Behavioral and Biochemical Effects of the NMDA Receptor Antagonists, MK-801 and Phencyclidine. Eur J Pharmacol. 1989; 166:359–366. [PubMed: 2553433]
67. Boyce S, Wyatt A, Webb JK, O'Donnell R, Mason G, Rigby M, Sirinathsinghji D, Hill RG, Rupniak NMJ. Selective NMDA NR2B antagonists induce antinociception without motor dysfunction: correlation with restricted localisation of NR2B subunit in dorsal horn. Neuropharmacology. 1999; 38:611–623. [PubMed: 10340299]
68. Loschmann PA, De Groote C, Smith L, Wullner U, Fischer G, Kemp JA, Jenner P, Klockgether T. Antiparkinsonian activity of Ro 25-6981, a NR2B subunit specific NMDA receptor antagonist, in animal models of Parkinson's disease. Exp Neurol. 2004; 187:86–93. [PubMed: 15081591]
69. Halgren TA. Merck molecular force field 0.1. Basis, form, scope, parameterization, and performance of MMFF94. J Comput Chem. 1996; 17:490–519.
70. Halgren TA. Merck molecular force field 0.2. MMFF94 van der Waals and electrostatic parameters for intermolecular interactions. J Comput Chem. 1996; 17:520–552.
71. Halgren TA. Merck molecular force field 0.3. Molecular geometries and vibrational frequencies for MMFF94. J Comput Chem. 1996; 17:553–586.
72. Halgren TA. Merck molecular force field 0.5. Extension of MMFF94 using experimental data, additional computational data, and empirical rules. J Comput Chem. 1996; 17:616–641.
73. Halgren TA, Nachbar RB. Merck molecular force field 0.4. Conformational energies and geometries for MMFF94. J Comput Chem. 1996; 17:587–615.
74. Traynelis SF, Burgess MF, Zheng F, Lyuboslavsky P, Powers JL. Control of voltage-independent zinc inhibition of NMDA receptors by the NR1 subunit. J Neurosci. 1998; 18:6163–6175. [PubMed: 9698310]
75. Junge CE, Sugawara T, Mannaioni G, Alagarsamy S, Conn PJ, Brat DJ, Chan PH, Traynelis SF. The contribution of protease-activated receptor 1 to neuronal damage caused by transient focal cerebral ischemia. Proc Natl Acad Sci U S A. 2003; 100:13019–13024. [PubMed: 14559973]
76. Kalinichev M, White DA, Hotlzman SG. Individual differences in locomotor reactivity to a novel environment and sensitivity to opioid drugs in the rat. I. Expression of morphine-induced locomotor sensitization. Psychopharmacology. 2004; 1777:61–67. [PubMed: 15316716]

77. Jorgensen WL. The Many Roles of Computation in Drug Discovery. Science. 2004; 303:1813–1818. [PubMed: 15031495]

78. Finlayson K, Turnbull L, January CT, Sharkey J, Kelly JS. [3H]Dofetilide binding to HERG transfected membranes: a potential high throughput preclinical screen. Eur J Pharmacol. 2001; 430:147–148. [PubMed: 11698075]

79. Greengrass P, Bremner R. Binding characteristics of 3H-prazosin to rat brain a-adrenergic receptors. Eur J Pharmacol. 1979; 55:323–326. [PubMed: 37098]

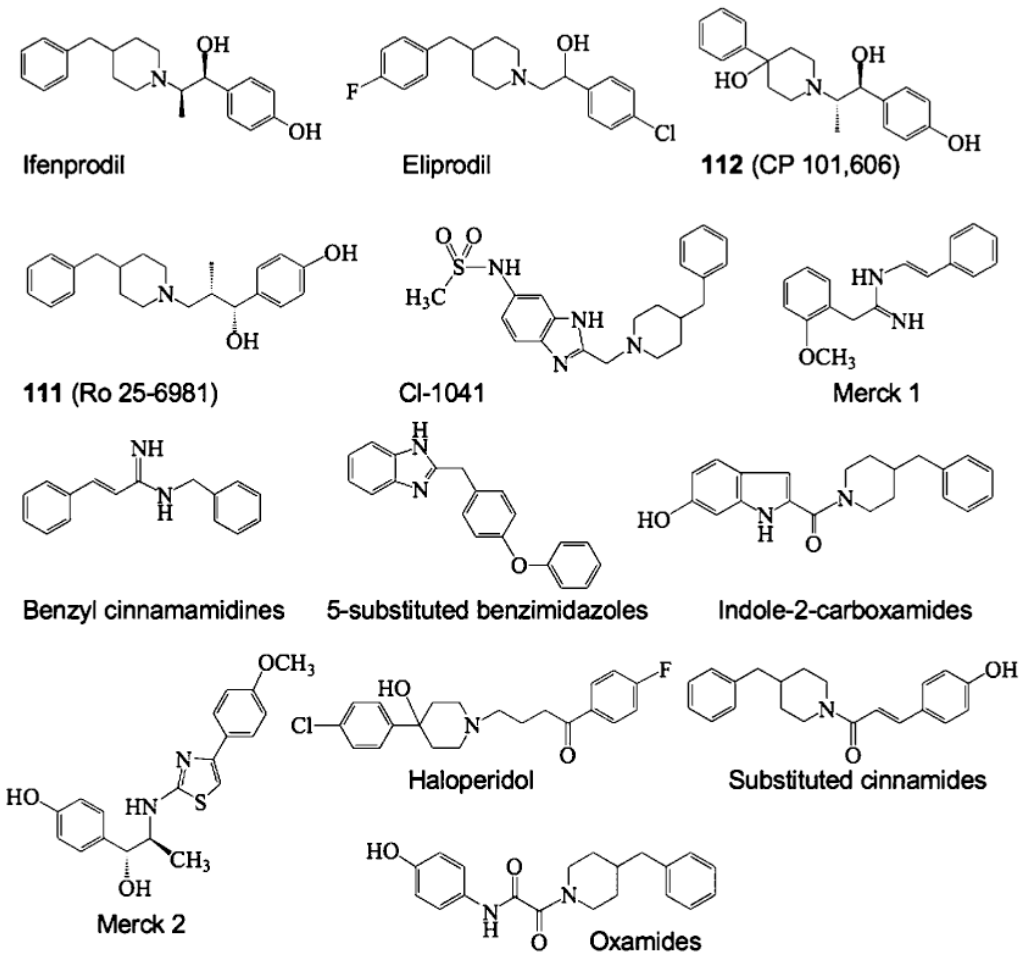

Figure 1.
The structures of prototypical NR2B-selective antagonists are shown.

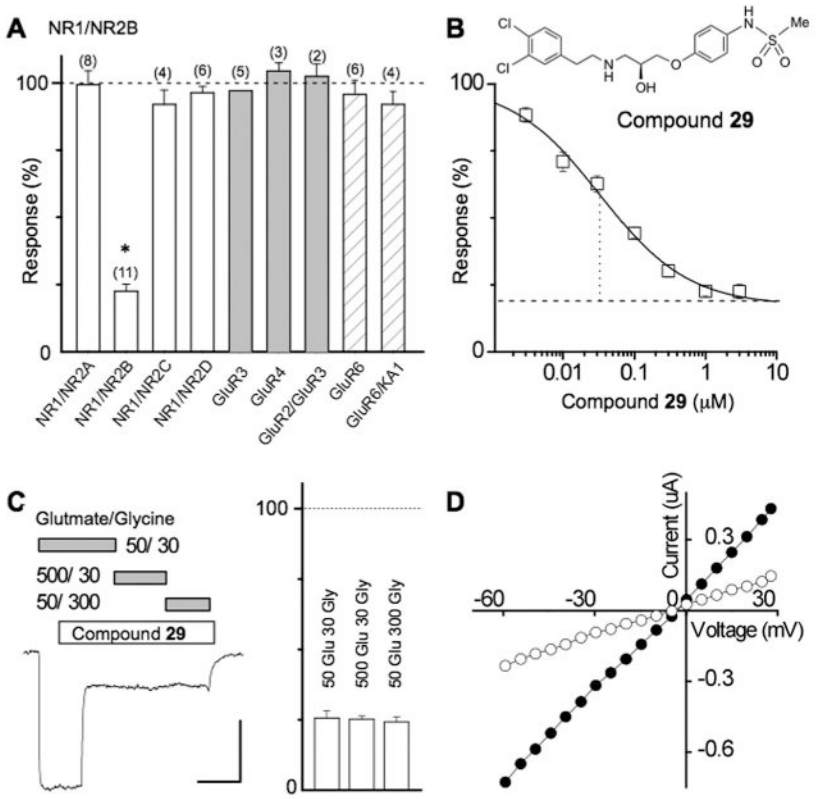

Figure 2.

Compound **29** is a potent, noncompetitive NR2B-selective antagonist. (A) Summary of the inhibition of evoked currents produced by 3 μM of **29** on recombinant glutamate receptors. NMDA receptor subunit combinations NR1/NR2A, NR1/NR2B, NR1/NR2C, and NR1/NR2D receptors were activated by 50 μM glutamate plus 30 μM glycine, AMPA receptor subnunit combinations GluR3, GluR4, and GluR2/3 receptors were activated by 50 μM kainate, kainate receptor subunit GluR6 was activated by 3 nM domoate, and kainate receptor subunit GluR6/KA1 receptors was activated by 100 μM AMPA. Data are expressed in all cases as percent of control evoked current. Holding potential was −40 mV in all cases. All values are mean ± SEM. Numbers in parentheses is number of oocytes; * indicates $p < 0.05$ (paired *t* test). (B) The structure of **29** is shown. A composite concentration–effect curve was generated in oocytes obtained from five different frogs and fitted as described in the Methods (V_{HOLD} −40 mV). The smooth curve is fitted by a logistic equation (see Methods); broken line shows fitted minimum response in saturating concentrations of **29**. The IC_{50} value determined from the composite average (33 nM) is similar to the average IC_{50} value determined from independent fits to data from each oocyte (50 nM). (C) Blockade by compound **29** is noncompetitive and cannot be surmounted by increasing concentrations of either glutamate or glycine (n = 3 oocytes each). (D) Block of NMDA receptor function by racemic **66**/**104** is independent of membrane potential.

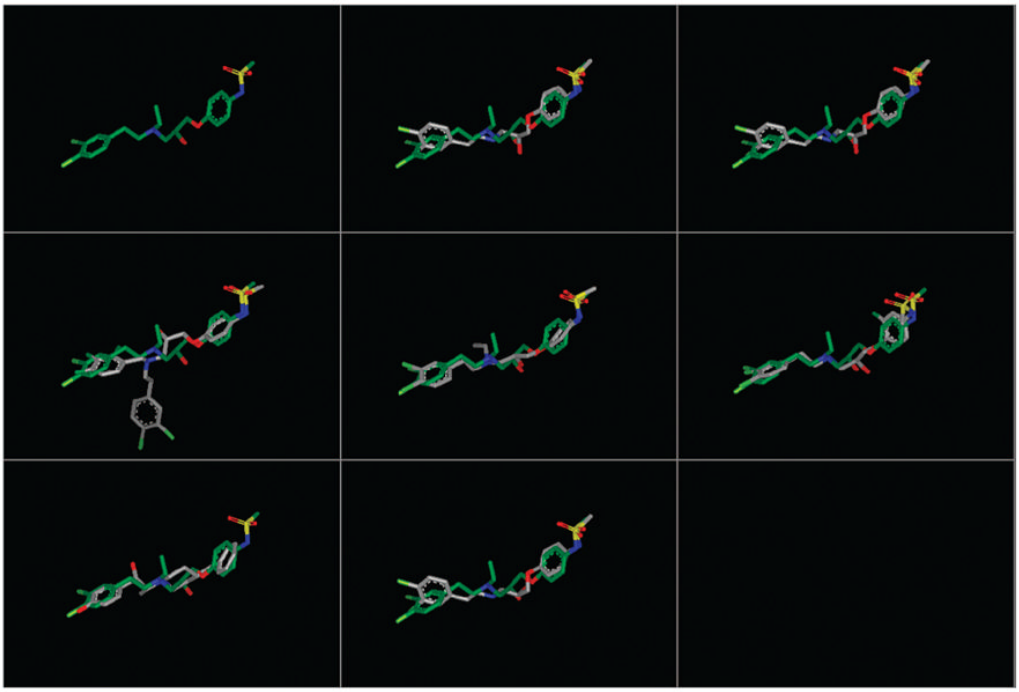

Figure 3.

Structural alignment to the query conformation of **67**. Each structure is represented by a conformer present in the conformer pool derived from OMEGA that provides the best combined alignment to the three-dimensional shape (ROCS) and electrostatic map (EON) **67** (green). Despite the significant electrostatic similarities between each compound and the query structure, compound **91** (middle left) and ifenprodil (bottom left) had a T_s below the threshold of significance. This is likely due to the additional aromatic substitution on **91** and the different scaffold of ifenprodil. The compounds are in the following order: top row, query, **52**, **29**; middle row, **91**, **67**, **30**; bottom row, ifenprodil, **103**.

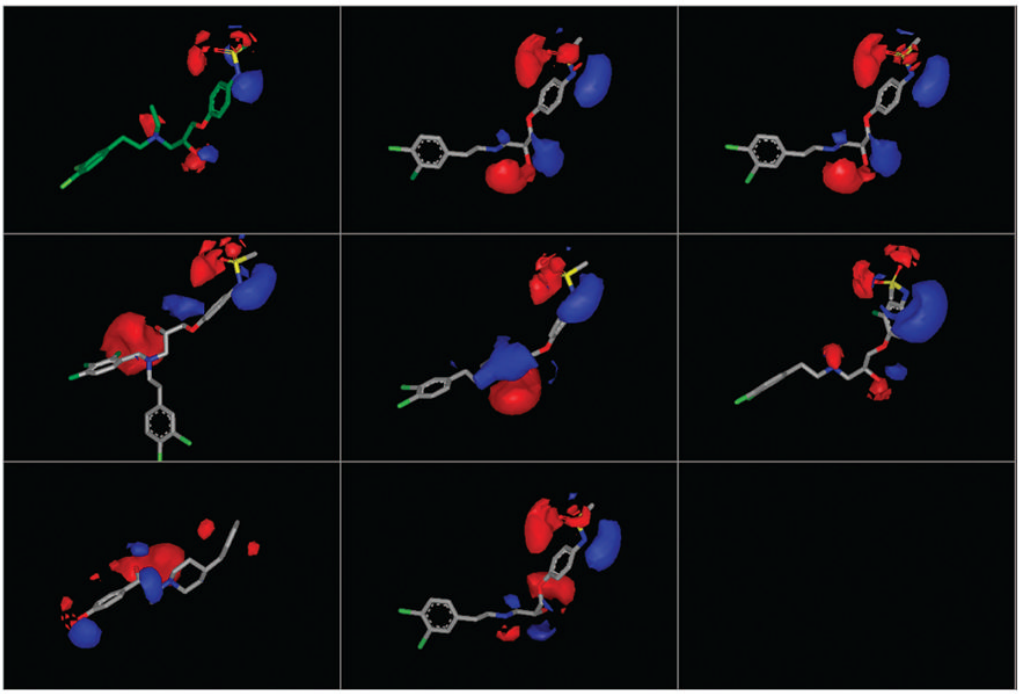

Figure 4.
Electrostatic potential maps (EON) of the fitted conformers depicted and ordered as in Figure 3. Despite structural variations within the propanolamine series and in ifenprodil, each compound displays a three-dimensional electrostatic profile similar to the query structure, even ifenprodil (bottom left), with a completely different scaffold than the propanolamines, achieves the threshold electrostatic similarity score of 0.2 when compared to the query structure.

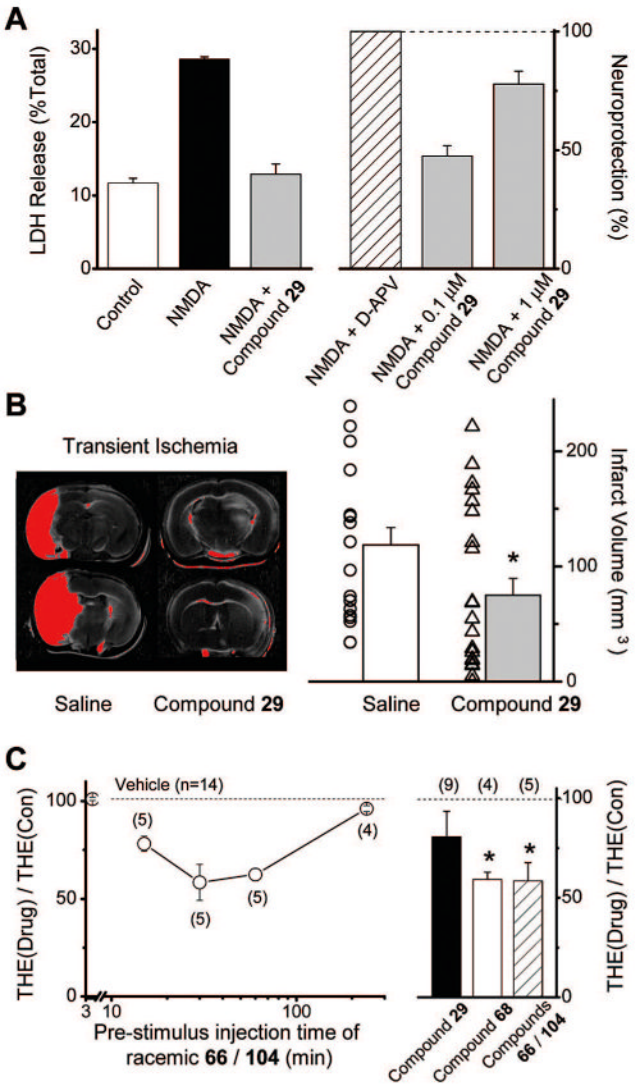

Figure 5.

Propanolamines are neuroprotective and anticonvulsant. (A) Left panel: NMDA induces release of LDH, which can be attenuated by 1 μM compound **29**. Right panel: compound **29** is neuroprotective in a concentration-dependent fashion in cortical cultures treated for 10 min with 100 μM NMDA. The neuroprotection produced by 100 μM D-APV was considered to be 100%. (B) Left panel: black and white scan of TTC stained 1 mm sections from C57B1/6 mice subjected to MCA occlusion for 30 min. Superimposed on this is a red digital threshold measurement of reductions of more than 30% average intensity of contralateral cortex. Animals were injected ip with vehicle (saline/DMSO) or compound **29** 30 min before MCA occlusion (see Methods). Right panel: summary of the reduction of infarct volume by 30 mg/kg compound **29** following transient focal ischemia. Individual data points show infarct volume from individual animals. Bar graph is mean ± SEM * indicates $p < 0.05$; Mann–Whitney test. (C) Left panel: ip injection of racemic mixture of **66/104** injected a variable time before stimulus caused a reduction in the duration of electroshock-induced tonic hindlimb extension. Right panel: summary of effects of 30 mg/kg compound **29**, **68**, **66/104** administered 30 min pre-electroshock simulus. Numbers in parenthesis indicate the number of rats tested. Symbols are mean ± SEM; * $p < 0.05$ (*t* test).

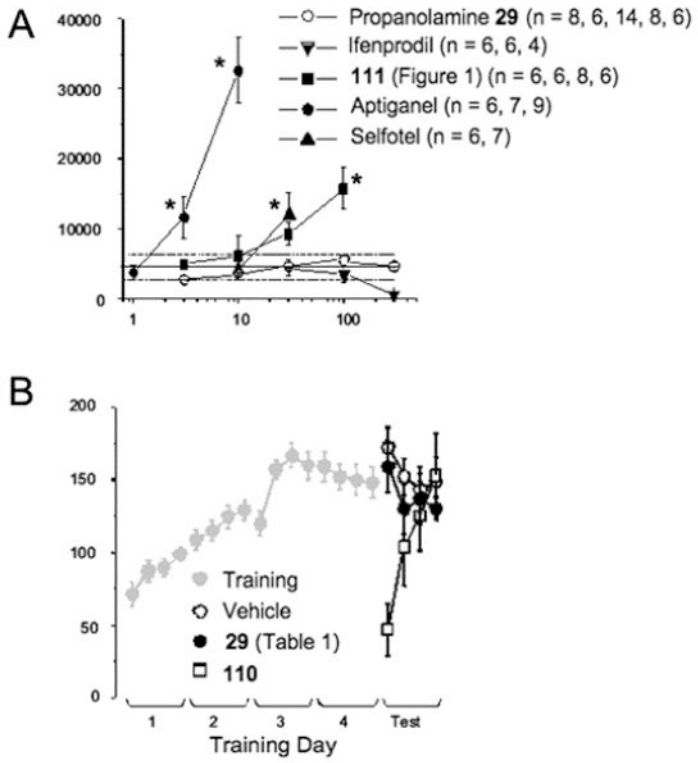

Figure 6.

Propanolamines do not alter locomotor activity or rotorod performance to the same extent as other similarly potent NMDA receptor antagonists. (A) The total horizontal activity following ip administration of the indicated dose of the test compounds is shown. The solid line shows the average of the response to vehicle injection; broken lines are the 95% confidence intervals for the vehicle injected animals. Each data point represents measurements from mean ±SEM (* indicates $p < 0.05$ from vehicle, ANOVA, post hoc Dunnett's). The number of animals tested per drug dose is indicated in the legend. (B) For rotorod, adult mice were placed on a rotating bar that was accelerated from 5 to 35 rpm over 5 min and the latency to fall was recorded for each animal (see Methods). Four trials (intertrial interval = 25 min) were run on five successive days. Training results for all mice shown in gray. On day five, the animals were randomly assigned to either vehicle control ($n = 5$), 0.3 mg/kg **110** ($n = 6$), or 30 mg/kg compound **29** ($n = 6$) delivered ip 20 min before the start of the first trial. Day 5 results represent the mean + SEM, *$p < 0.05$ from control by ANOVA, posthoc Dunnett's.

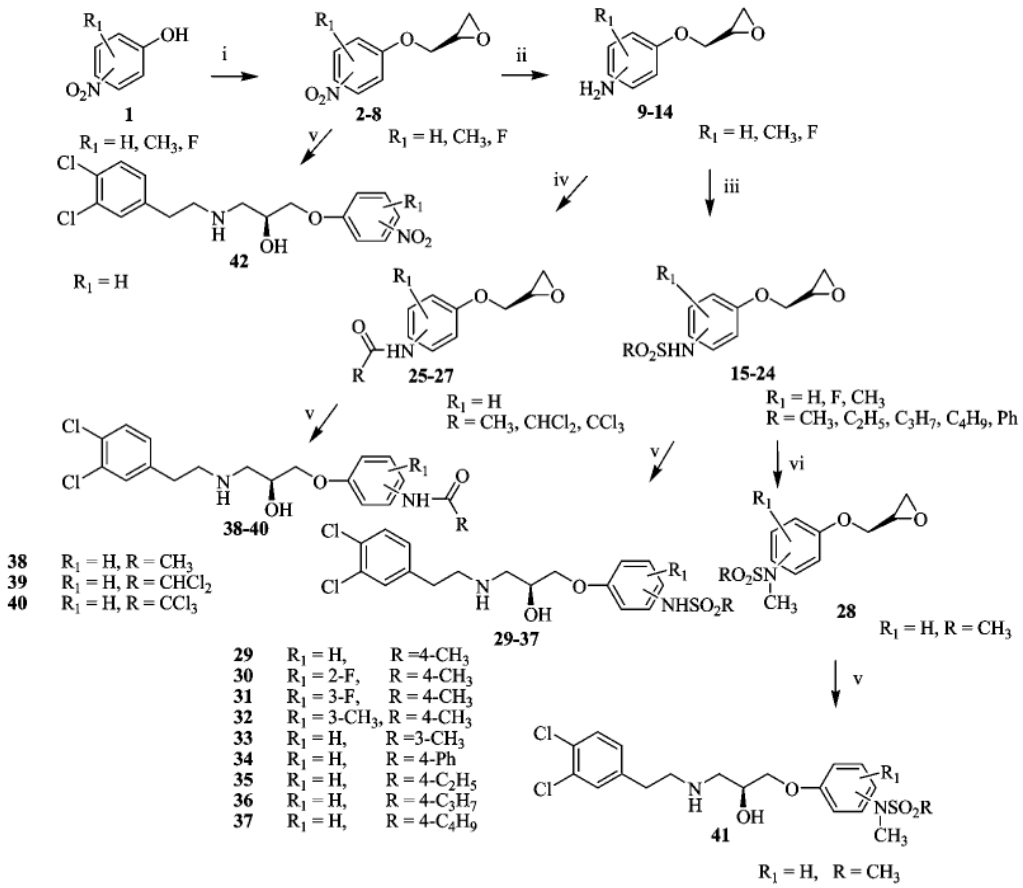

Scheme 1a.

[a] (i) Glycidyl nosylate, cesium fluoride in DMF, r.t.; (ii) H_2, poisoned Pd/C, in THF, r.t.; (iii) RSO_2Cl, DIEA, DCM, 0°C; (iv) RCOCl, DIEA, DCM, 0 °C; (v) 3,4-dichlorophenylethylamine, EtOH, reflux; (vi) CH_3-I, K_2CO_3, acetone, r.t.

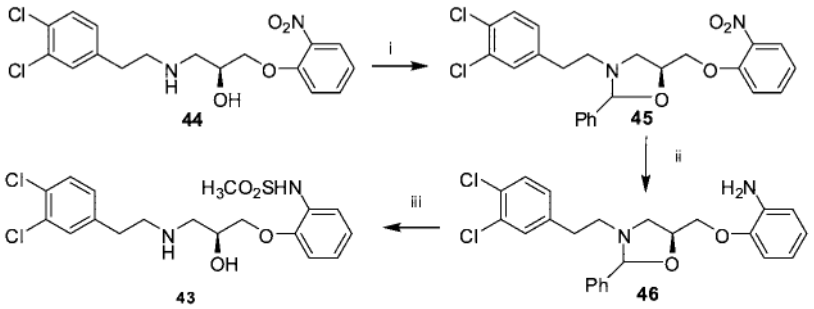

Scheme 2a.

[a] (i) Benzaldehyde, *p*-toluenesulfonic acid, toluene, reflux; (ii) Pd/C (%10), 2N NaOH, ethanol; (iii) CH_3SO_2Cl, DIEA, DCM, 0°C, 1N HCl.

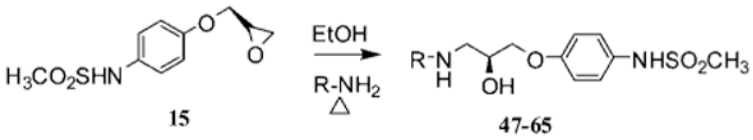

Scheme 3.

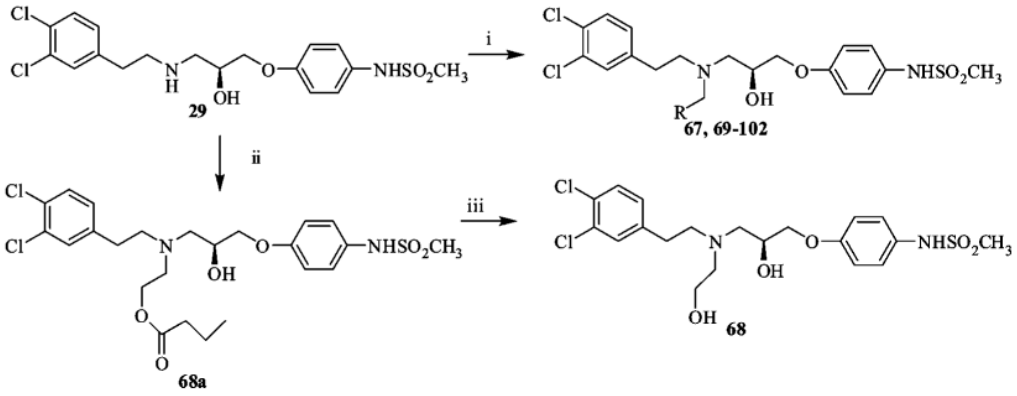

Scheme 4a.

[a] (i) R-CHO, $NaB(OAc)_3H$, 1,2-dichloroethane, r.t.; (ii) *O*-butyryl glycoaldehyde, $NaB(OAc)_3H$, 1,2-dichloroethane, r.t.; (iii) NaOMe, MeOH, r.t.

Table 1

IC_{50} Values of Propanolamine NR1/NR2B Receptor Antagonists from Variations in the Phenoxy Ring

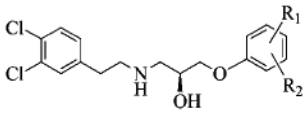

compd	R_1	R_2	IC_{50} (±95% CI) (μM)[a]	N
29	H	4-$NHSO_2CH_3$	0.050 (0.037, 0.068)	53
30	2-F	4-$NHSO_2CH_3$	0.072 (0.052, 0.100)	12
31	3-F	4-$NHSO_2CH_3$	0.427 (0.340, 0.535)	11
32	3-CH_3	4-$NHSO_2CH_3$	0.687 (0.479, 0.986)	11
33	H	3-$NHSO_2CH_3$	0.530 (0.221, 1.27)	14
34	H	4-$NHSO_2Ph$	1.45 (0.206, 10.2)	8
35	H	4-$NHSO_2C_2H_5$	0.587 (0.480, 0.719)	12
36	H	4-$NHSO_2C_3H_7$	6.10 (4.31, 8.63)	4
37	H	4-$NHSO_2C_4H_9$	6.79 (5.01, 9.23)	4
38	H	4-$NHCOCH_3$	4.37 (1.81, 10.5)	3
39	H	4-$NHCOCHCl_2$	12.8 (9.06, 17.9)	4
40	H	4-$NHCOCCl_3$	10.6 (7.43, 15.3)	4
41	H	4-$N(CH_3)SO_2CH_3$	9.91 (3.49, 28.1)	15
42	H	4-NO_2	9.38 (5.77, 15.2)	12
43	H	2- $NHSO_2CH_3$	12.0 (5.23, 27.6)	17

[a]For all compounds in all tables, the mean IC_{50} value was determined from the fitted concentration-effect curves from individual *Xenopus laevis* oocytes recorded under two electrode voltage clamp; oocytes expressed recombinant rat NR1/NR2B receptors. The 95% confidence intervals (CI) determined from log(EC_{50} values), which has a normal distribution. N is the number of oocytes recorded.

Table 2

IC_{50} Values of Propanolamine NR1/NR2B NMDA Receptor Antagonists Derived from Variations in the Amino Substitution

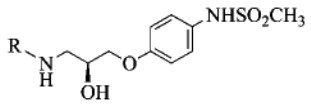

compd	R	IC_{50} (±95% CI) (μM)	N
29	$3,4Cl_2C_6H_3(CH_2)_2$	0.050 (0.037, 0.068)	53
47	$2ClC_6H_4(CH_2)_2$	0.429 (0.352, 0.522)	16
48	$3ClC_6H_4(CH_2)_2$	0.628 (0.515, 0.767)	11
49	$4ClC_6H_4(CH_2)_2$	0.101 (0.080, 0.126)	10
50	$2,4Cl_2C_6H_3(CH_2)_2$	2.317 (0.726, 7.40)	17
51	$3Cl\text{-}4FC_6H_3(CH_2)_2$	0.397 (0.346, 0.456)	30
52	$4Cl\text{-}3FC_6H_3(CH_2)_2$	0.068 (0.056, 0.082)	16
53	$2FC_6H_4(CH_2)_2$	0.573 (0.504, 0.653)	11
54	$3FC_6H_4(CH_2)_2$	0.853 (0.643, 1.13)	16
55	$4FC_6H_4(CH_2)_2$	0.748 (0.582, 0.964)	12
56	$3,4F_2C_6H_3(CH_2)_2$	0.357 (0.308, 0.415)	22
57	$2OHC_6H_4(CH_2)_2$	2.00 (1.71, 2.33)	4
58	$3OHC_6H_4(CH_2)_2$	4.43 (3.40, 5.75)	5
59	$4OHC_6H_4(CH_2)_2$	7.24 (4.33, 12.1)	4
60	$3,5(OH)_2C_6H_2(CH_2)_2$	>100	4
61	$3,4(OH)_2C_6H_2(CH_2)_2$	>100	4
62	$3,4(OCH2O)C_6H_2(CH_2)_2$	0.951 (0.746, 1.21)	9
63	$3,4(CH_3)_2C_6H_3(CH_2)_2$	0.207 (0.145, 0.295)	12
64	1-naphthyl-$CH(CH_3)$	5.07 (2.06, 12.5)	13
65	$4\text{-}NO_2C_6H_4(CH_2)_2$	1.14 (0.804, 1.63)	10

Table 3

IC_{50} Values of Propanolamine NR1/NR2B NMDA Receptor Antagonists Derived from Variations in the Amino Alkyl Substitution

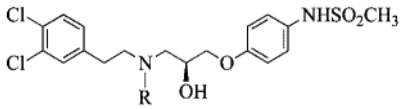

compd	R	IC_{50} (±95% CI) (μM)	N
29	H	0.050 (0.037, 0.068)	53
66	CH3	0.130 (0.091, 0.186)	41
67	C_2H_5	0.096 (0.065, 0.143)	29
68	C_2H_4OH	0.122 (0.091, 0.163)	38
69	C_3H_7	0.635 (0.481, 0.841)	25
70	C_4H_9	0.421 (0.345, 0.512)	46
71	C_5H_{11}	0.659 (0.463, 0.938)	10
72	$(CH_3)_2CHCH_2$	1.27 (0.975, 1.65)	30
73	$C_6H_{11}CH_2$	9.84 (3.88, 24.9)	33
74	$CH(CH_3)_2$	0.603 (0.497, 0.731)	12
75	$C_6H_5CH_2$	0.177 (0.116, 0.271)	24

Table 4

IC_{50} Values of Propanolamine NR1/NR2B NMDA Receptor Antagonists Derived from Variations in the Aminomethylaromatic Substitution

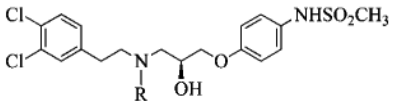

compd	R	I_{50} (±95% CI) (μM)	N
75	$C_6H_5CH_2$	0.177 (0.116, 0.271)	24
76	2-$OHC_6H_4CH_2$	0.662 (0.451, 0.973)	45
77	3-$OHC_6H_4CH_2$	0.238 (0.197, 0.289)	47
78	4-$OHC_6H_4CH_2$	0.113 (0.095, 0.133)	13
79	2,3-$(OH)_2C_6H_3CH_2$	1.82 (1.23, 2.71)	9
80	2,4-$(OH)_2C_6H_3CH_2$	0.146 (0.099, 0.215)	11
81	2-$OCH_3C_6H_4CH_2$	3.86 (0.622, 24.04)	4
82	2,3-$(OCH_3)_2C_6H_3CH_2$	2.79 (1.65, 4.71)	17
83	2,6-$(OCH_3)_2C_6H_3CH_2$	11.9 (7.9, 17.8)	11
84	2,3-(-OCH_2O-) $C_6H_3CH_2$	5.01 (2.09, 12.0)	4
85	2-$ClC_6H_4CH_2$	0.479 (0.406, 0.565)	14
86	2-$BrC_6H_4CH_2$	0.038 (0.033, 0.045)	8
87	2-$FC_6H_4CH_2$	0.080 (0.049, 0.130)	22
88	3-$FC_6H_4CH_2$	0.249 (0.179, 0.347)	16
89	4-$FC_6H_4CH_2$	0.275 (0.110, 0.682)	15
90	2,6-$F_2C_6H_3CH_2$	0.281 (0.145, 0.546)	12
91	2,3,4-$F_3C_6H_2CH_2$	0.051 (0.029, 0.087)	14
92	2,3,4,5,6-F_5PhCH_2	0.524 (0.419, 0.655)	31
93	2-$CH_3C_6H_4CH_2$	5.70 (4.08, 7.96)	22
94	4-$CH_3C_6H_4CH_2$	5.41 (2.88, 10.1)	18
95	2-$CF_3C_6H_4CH_2$	3.72 (2.06, 6.71)	21
96	2-$NO_2C_6H_4CH_2$	0.589 (0.399, 0.869)	6
97	2(CH_3COO) $C_6H_4CH_2$	0.500 (0.376, 0.665)	12
98	2-pyridylCH_2	2.76 (2.15, 3.55)	12
99	3-pyridylCH_2	0.278 (0.233, 0.332)	21
100	2-thiazolylCH_2	3.58 (3.02, 4.26)	19
101	$C_6H_5(CH_2)_2$	3.51 (2.08, 5.93)	6
102	2-$OHC_6H_4(CH_2)_2$	0.755 (0.592, 0.964)	12

Table 5

IC_{50} Values of Propanolamine NR1/NR2B NMDA Receptor Antagonists Derived from Variations in the Stereochemistry

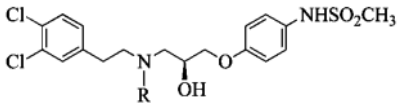

compd	stereochemistry	R	IC_{50} (±95% CI) (μM)	N
29	S	H	0.050 (0.037, 0.068)	53
103	*R*	H	0.188 (0.128, 0.277)	10
66	*S*	CH_3	0.130 (0.091, 0.186)	41
104	*R*	CH_3	0.253 (0.211, 0.303)	11
68	*S*	C_2H_4OH	0.122 (0.091, 0.163)	38
105	*R*	C_2H_4OH	0.173 (0.146, 0.205)	12
70	*S*	C_4H_9	0.421 (0.345, 0.512)	46
106	*R*	C_4H_9	1.28 (1.06, 1.54)	39
76	*S*	2-$OHC_6H_4CH_2$	0.662 (0.451, 0.973)	45
107	*R*	2-$OHC_6H_4CH_2$	0.433 (0.309, 0.605)	44
77	*S*	3-$OHC_6H_4CH_2$	0.238 (0.197, 0.289)	47
108	*R*	3-$OHC_6H_4CH_2$	0.409 (0.327, 0.512)	13

Table 6
Highest Scoring Conformation for Each Molecule from EON Comparison

name	IC_{50} (μM)	electrostatic Tanimoto score (T_e)	shape Tanimoto score (T_s)
52	0.065	0.47	0.72
29	0.037	0.47	0.71
91	0.064	0.41	0.54
103	0.219	0.36	0.72
67	0.089	0.36	0.703
30	0.058	0.32	0.71
ifenprodil	0.073	0.20	0.68

Table 7
hERG and αl-Adrenergic Receptor Binding of Selected Propanolamines

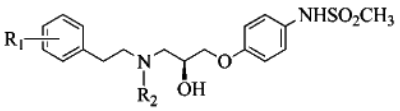

compd	R_1	R_2	hERG IC_{50}(μM)	α1-AdR IC_{50}(μM)
29	3,4-Cl_2	H	0.73	2.4
49	4-Cl	H	1.39	9.5
52	4-Cl, 3-F	H	1.91	>10
56	3,4-F_2	H	1.63	>10
63	3,4-$(CH_3)_2$	H	2.4	2.2
66	3,4-Cl_2	CH_3	0.37	1.4
67	3,4-Cl_2	C_2H_5	0.17	3.5
69	3,4-Cl_2	C_3H_7	0.13	nd
70	3,4-Cl_2	C_4H_9	0.07	4.9
72	3,4-Cl_2	$(CH_3)_2CHCH_2$	0.37	>10
75	3,4-Cl_2	$C_6H_5CH_2$	0.43	>10
76	3,4-Cl_2	2-$OHC_6H_4CH_2$	0.83	>10
77	3,4-Cl_2	3-$OHC_6H_4CH_2$	0.78	>10
87	3,4-Cl_2	2-$FC_6H_4CH_2$	1.2	>10
91	3,4-Cl_2	2,3,4-$F_3C_6H_4CH_2$	1.7	>10